Published in "Palaeogeography, Palaeoclimatology, Palaeoecology
doi: 10.1016/j.palaeo.2012.11.003 , 2012"
which should be cited to refer to this work.

Neritic isotope and sedimentary records of the Eocene–Oligocene greenhouse–icehouse transition: The Calcare di Nago Formation (northern Italy) in a global context

David Jaramillo-Vogel [a,*], André Strasser [a], Gianluca Frijia [b], Silvia Spezzaferri [a]

[a] Department of Geosciences, University of Fribourg, 1700 Fribourg, Switzerland
[b] Institut für Erd- und Umweltwissenschaften, University of Potsdam, 14476 Potsdam, Germany

From the Middle Eocene to Early Oligocene, the Earth experienced the most significant climatic cooling of the Cenozoic era. The Eocene–Oligocene transition (EOT) represents the culmination of this climatic cooling, leading to the onset of the Antarctic glaciation and, consequently, to the beginning of the present-day icehouse world. Whereas the response of deep-sea systems to this climate transition has been widely studied, its impact on the shallow-water carbonate realm is poorly constrained. Here, the sedimentary expression of the EOT in two shallow-marine carbonate successions (Nago and San Valentino, northern Italy) belonging to the Calcare di Nago Formation is presented. The chronostratigraphic framework was constructed by integrating litho-, bio-, and isotope-stratigraphic data (C and Sr isotopes), allowing to correlate these shallow-marine successions with pelagic sections in central Italy (Massignano), Tanzania (TDP Sites 12 and 17), and the Indian Ocean (ODP Site 744). Within several sections in northern Italy, including Nago and San Valentino, a Priabonian (Late Eocene) transgression is recorded. Oxygen isotopes of ODP Site 744 show a coeval negative shift of 0.4‰, suggesting a glacio-eustatic origin for this transgression. In the Nago and San Valentino sections, no prominent sequence boundary has been detected that would indicate a rapid sea-level drop occurring together with the positive shift in $\delta^{18}O$ defining the EOT-1 cooling event. Instead, a gradual shallowing of the depositional environment is observed. At TDP Sites 12 and 17, the EOT-1 is followed by a negative shift in $\delta^{18}O$ of around 0.4‰, which correlates with a relative deepening of the environment in the studied sections and suggests a melting pulse between EOT-1 and the Oligocene isotope event 1 (Oi-1). The positive $\delta^{18}O$ shift related to the Oi-1 translates in San Valentino into a change in carbonate factory from a photozoan association dominated by larger benthic foraminifera, corals, and red algae to a heterozoan association dominated by bryozoans. The same bryozoan facies occurs in several Italian localities near the Eocene–Oligocene boundary. This facies is interpreted to represent an analogue of modern cool-water carbonates and results from a cooling pulse of at least regional scale, associated to the Oi-1 event.

1. Introduction

The Eocene–Oligocene transition (EOT) marks the transition between a greenhouse and an icehouse world. In deep-sea records, it is expressed by prominent positive shifts in stable oxygen- and carbon-isotope values (Kennett and Shackleton, 1976; Miller et al., 1991; Zachos et al., 1996, 2001; Coxall and Pearson, 2007; Coxall and Wilson, 2011). The positive shift of oxygen isotopes occurred in two steps: a precursor step (~0.5‰) leading to the EOT-1 event (Katz et al., 2008), and a second, more pronounced step (~1‰) leading to the Oligocene isotope event 1 (Oi-1), also referred to as the Eocene–Oligocene glacial maximum (EOGM). The duration of this shift is estimated at around 500 kyr (Coxall et al., 2005; Coxall and Pearson, 2007; Katz et al., 2008; Miller et al., 2008; Coxall and Wilson, 2011; Wade et al., 2012). An additional but less clear precursor step has been reported only from the St. Stephen Quarry in Alabama (Katz et al., 2008; Miller et al., 2009). The Eocene–Oligocene boundary (Global Boundary Stratotype Section and Point = GSSP) as defined at Massignano (Italy) by the last appearance of the planktonic foraminifer *Hantkenina* (Nocchi et al., 1988; Premoli Silva and Jenkins, 1993) occurs within the EOT. The GSSP falls within magnetochron C13r but cannot be correlated to any stable isotope event.

While it is widely accepted that large ice sheets first formed in Antarctica during the EOT, there is increasing evidence that smaller transient glaciations already occurred during the Middle and Late Eocene (Tripati et al., 2005; Peters et al., 2010; Dawber et al., 2011). However, fluctuations in oxygen-isotope composition measured in deep-sea sediments do not allow differentiating between changes in temperature, salinity, and ice-volume, and alone do not permit to

* Corresponding author. Tel.: +41 263008979; fax: +41 263009742.
E-mail address: david.jaramillovogel@unifr.ch (D. Jaramillo-Vogel).

reconstruct in detail the formation of ice-sheets in Antarctica. Shallow-marine successions, on the other hand, where changes in water depth affect sedimentation, can be used to reconstruct local and regional sea-level history. Where such relative sea-level changes occur together with global shifts in oxygen isotopes, they can be interpreted in terms of glacio-eustatic sea-level fluctuations linked to waxing and waning of glaciers and ice sheets. In this respect, neritic deposits have been studied on the New Jersey shelf (Pekar et al., 2002; Miller et al., 2005a, 2009), at St. Stephens Quarry in Alabama (Katz et al., 2008; Miller et al., 2008, 2009; Wade et al., 2012) (Fig. 1A), and in Priabona in northern Italy (Houben et al., 2012) (Fig. 1A and B). However, due to the scarce and often incomplete shallow-water records spanning the EOT, open questions regarding the climatic and oceanographic evolution during this time interval remain.

Neritic carbonates are an excellent proxy to monitor environmental changes: carbonate-producing organisms react sensitively to changes in the environment (e.g., water depth, light intensity, nutrient input, water temperature, hydrodynamic energy). However, the correlation of shallow benthic biozones with stable-isotope, magneto-, and calcareous-plankton stratigraphy from pelagic sections, where the EOT has been characterized, is not free of uncertainties (Brinkhuis, 1994; Brinkhuis and Visscher, 1995; Luciani et al., 2002; Cascella and Dinarès-Turell, 2009; Agnini et al., 2011). One problem is the relatively poor chronostratigraphic resolution attained by benthic foraminiferal

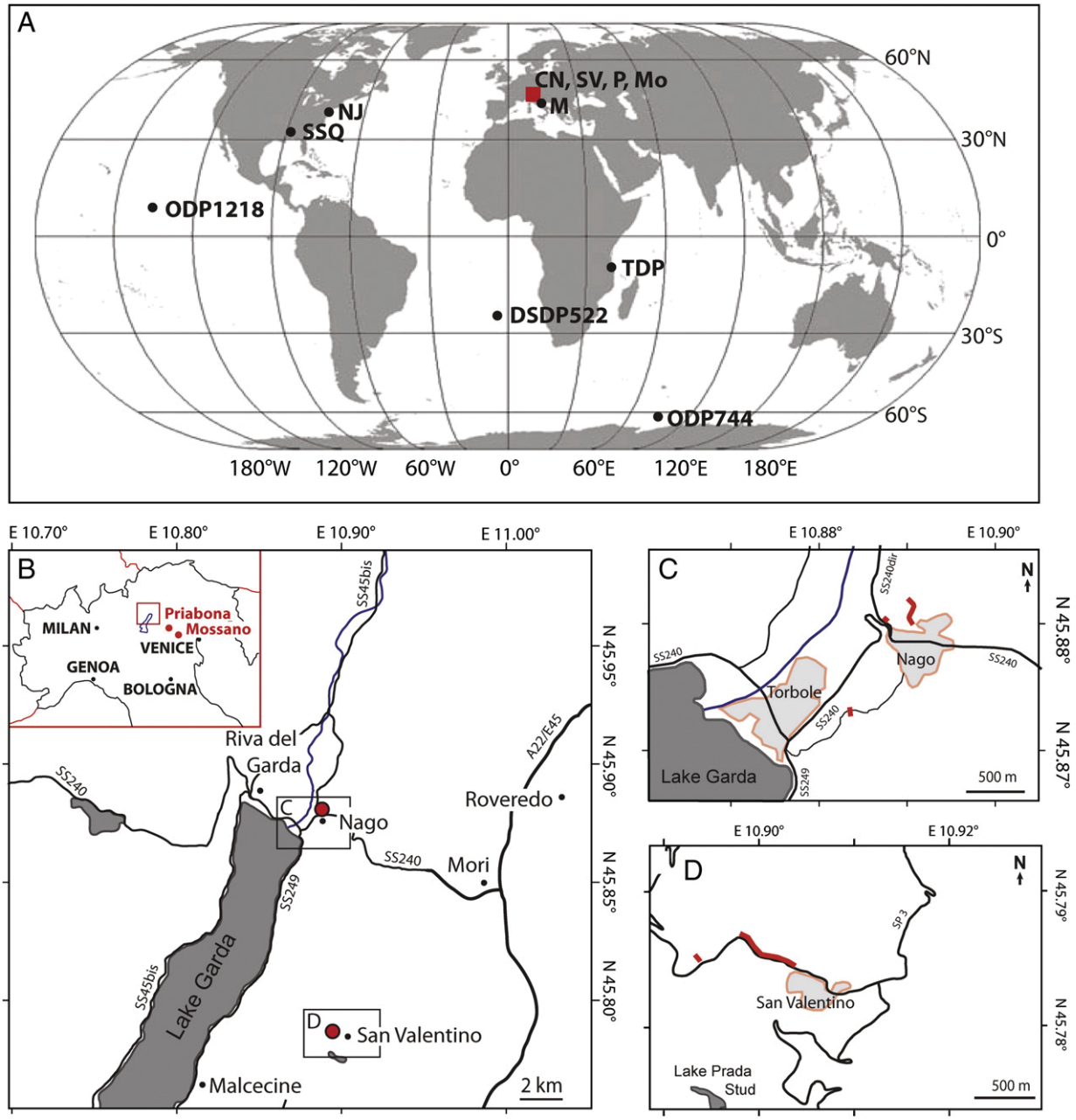

Fig. 1. A) Location of the studied sections in northern Italy (red square) and of other localities mentioned in this study containing the Eocene–Oligocene transition: Nago (CN), San Valentino (SV), Massignano (M), Priabona (P), Mossano (Mo), St. Stephens Quarry (SSQ), New Jersey shelf (NJ), Tanzania Drilling Project (TDP), ODP Sites 744 and 1218, and DSDP Site 522. B) Map of northern Italy showing the location of the Priabonian type locality at Priabona (Monti Lessini) and the Mossano section (Colli Berici). The magnification of the red square shows the area with the studied sections. C and D) Location of the measured sections in Nago and San Valentino, respectively. Red lines represent the measured sections. (For interpretation of the references to colour in this figure legend, the reader is referred to the web of this article.)

biostratigraphy. In addition, carbonate platforms declined rapidly during the Late Eocene and earliest Oligocene (Adams et al., 1986; Papazzoni and Sirotti, 1995; Kiessling et al., 2003; Nebelsick et al., 2005), thus offering fewer possibilities to constrain the EOT in shallow depositional environments.

Here, we present a dataset integrating lithofacies analysis with biostratigraphic and isotope-stratigraphic (C and Sr) data obtained from two Late Eocene to Early Oligocene shallow-marine sections belonging to the Calcare di Nago Formation (northern Italy, Fig. 1B,C,D). Based on these data a high-resolution correlation with pelagic successions from the Tethys (Massignano), Tanzania (TDP Sites 12 and 17), and the southern Indian Ocean (ODP Site 744) (Fig. 1A) is proposed. The aim of this study is to compare the lithofacies evolution observed in the shallow-marine sections with geochemical and micropalaeontological data from the pelagic realm, and to characterize the EOT in the Calcare di Nago Formation. This study is relevant because it tracks the timing of the onset of the Antarctic glaciation in a carbonate neritic depositional environment and reveals how carbonate-producing biota reacted to a greenhouse–icehouse transition.

2. Geological and stratigraphical setting

The studied sections are located near the villages of Nago and San Valentino, on the northeastern side of Lake Garda (northern Italy; Figs. 1B,C,D). Both successions belong to the Calcare di Nago Formation (Castellarin and Cita, 1969a), which was deposited on the western margin of the Lessini Shelf, a Tertiary carbonate platform superimposed on the Jurassic Trento platform (Bosellini, 1989; Luciani, 1989). According to Meulenkamp and Sissingh (2003), the Lessini Shelf was located within the subtropical belt at around 36° to 38°N during the Late Eocene. Sediments were deposited in open-marine conditions and are mainly composed of coralline red algae, larger benthic foraminifera, and corals (Luciani, 1989; Bassi, 1998; Bosellini, 1998).

Within the Nago section, Luciani (1989) recognized two large-scale shallowing-up cycles, which in turn are superimposed by several smaller-scale cycles. Based on larger foraminifera biostratigraphy, the lower large-scale cycle (Luciani, 1989; Papazzoni and Sirotti, 1995) was interpreted to have been deposited in the Middle Eocene (*Nummulites lyelli*, *N. biedai* and *N. variolarius/incrassatus* zones, Bartonian), while the upper cycle was attributed to the Late Eocene (*Nummulites fabianii* s.s. zone, Priabonian). The interval studied in San Valentino was interpreted to have been deposited during the Early and Late Priabonian based on the recognition of the *N. fabianii* and *N. retriatus* zones (Castellarin and Cita, 1969a).

Although the Calcare di Nago Formation is mainly composed of shallow-water carbonates, scarce planktonic foraminifera allow refining the biostratigraphy. At the base of the Nago section (10 m; Fig. 2), *Morozovella spinulosa* was recognized, which indicates zones P14 (Berggren et al., 1995) and E13 (Berggren and Pearson, 2005). The occurrence of *M. spinulosa* is in agreement with the Bartonian age proposed by Luciani (1989) and Papazzoni and Sirotti (1995) for the lower part of the section.

In the upper part of the Nago section, *Turborotalia cunialensis* was found at metre 68, around metre 95, and at metre 140 (Fig. 2). *T. cunialensis* occurs within zones P16–17 (Berggren et al., 1995) and E15–E16 (Berggren and Pearson, 2005) in the latest Eocene. In the Massignano section, which includes the GSSP for the Eocene–Oligocene boundary, the first appearance datum (FAD) of this foraminifer occurs at metre 7.5 (Spezzaferri et al., 2002) and is dated at 35.2 Ma (Jovane et al., 2007), while the last appearance datum (LAD) occurs 40 cm below the Eocene–Oligocene boundary, dated at 33.765 Ma (Berggren et al., 1995). Although these data do not permit the placement in the Nago section of the Eocene–Oligocene boundary as defined in Massignano, they imply that the rocks occurring between metres 68 and 140 were deposited during the latest Eocene.

In San Valentino, orthophragminids (*Discocyclina* and *Asterocyclina*) are present in almost the entire section, in contrast to other larger benthic foraminifera like *Nummulites*, *Pellatispira*, *Heterostegina*, *Operculina* and *Spiroclypeus* that seem to be much more facies dependent. However, orthophragminids decrease rapidly above metre 110.8 where tests are often filled with glauconite and abraded. The last debris of *Discocyclina* and *Asterocyclina* was found at 114.8 m, implying that these genera disappeared somewhere between 110.8 m and 114.8 m within bryozoan-dominated beds. Therefore, we tentatively place their extinction level at metre 113.5 where the last moderately well-preserved specimens are found. This extinction is followed by an interval of around 2 m containing up to 90% bryozoans (in absence of larger benthic foraminifera and red algae). Above this interval red algae, *Nummulites*, and *Operculina* reoccur.

The Eocene–Oligocene boundary in the Lessini Shelf and the Colli Berici areas is marked by the occurrence of bryozoan marls and limestones (Castellarin and Cita, 1969b; Ungaro, 1978; Setiawan, 1983; Barbin, 1988; Trevisani, 1997; Nebelsick et al., 2005). Interestingly, in three sections outcropping in the Priabonian region including the Priabonian type locality (Priabona, Buco della Rana and Bressana; around 40 km to the east of San Valentino), Setiawan (1983) reported the last occurrence of *Discocyclina* and *Asterocyclina* at the transition from larger benthic foraminifera to bryozoan dominated deposits (between microfacies units IV and V in Priabona, XI and XII in Buco della Rana and III and IV in Bressana). Similar as in San Valentino this extinction is followed by an interval completely dominated by bryozoans (up to 100%). Above this interval, *Operculina* and *Nummulites* reoccur. At the Val D'Ir (15 km north of San Valentino), Castellarin and Cita (1969b) found bryozoan marls and limestones corresponding to the transition between the Calcare di Nago and the Marne di Bolognano formations. Similar to the observations made in San Valentino and the Priabona area (Setiawan, 1983), they also report broken discocyclinids at the base of a bryozoan limestone, which then completely disappear. This implies that at least regionally the extinction of *Discocyclina* and *Asterocyclina* occurring together with the establishment of bryozoan beds as observed in San Valentino can be unequivocally used for correlation (Fig. 3).

Brinkhuis (1994) and Brinkhuis and Visscher (1995), by means of dinoflagellate cyst stratigraphy, were able to correlate the shallow-marine deposits of the Priabonian type locality (eastern Lessini Shelf, Fig. 1B) with pelagic sections of central Italy, including Massignano (Fig. 3). Following their correlation, the Eocene–Oligocene boundary as defined in Massignano occurs in the middle of the Priabonian type section. The bryozoan beds occur about 10 m above the transposed Eocene–Oligocene boundary in the upper part of the Gse and the lower part of the Adi dinoflagellate cyst zones (Brinkhuis, 1994). This implies that the bryozoan beds and extinction of discocyclinids in the Priabonian type locality occurred within the Early Oligocene, which is in agreement with observations made in Tanzania where the LAD of *Discocyclina* shortly postdates the Eocene–Oligocene boundary (Cotton and Pearson, 2011).

Based on the FAD of the characteristic Priabonian larger benthic foraminifera *Nummulites fabianii*, *N. stellatus,* and *Spiroclypeus carpaticus,* Papazzoni and Sirotti (1995) correlated the transgression occurring at metre 52 in the Nago section to the one recorded at the base of the Priabonian type section and to the one occurring between the Calcari Nummulitici and Marne di Priabona formations at Mossano (Fig. 1B). Luciani et al. (2002) have shown that the first occurrence of *N. fabianii* at the Calcari Nummulitici–Marne di Priabona transition in Mossano corresponds to the upper part of the planktonic foraminiferal zone P15 (Berggren et al., 1995) and the nannofossil zone NP18 (Martini, 1971) and, therefore, lies within the Late Eocene. Additionally, these authors noticed that 8 m above this transition the rocks are already referable to P16, which characterizes the latest Eocene. Therefore, the existence of a hiatus or of condensed levels at this transition in Mossano seems likely (Luciani et al., 2002).

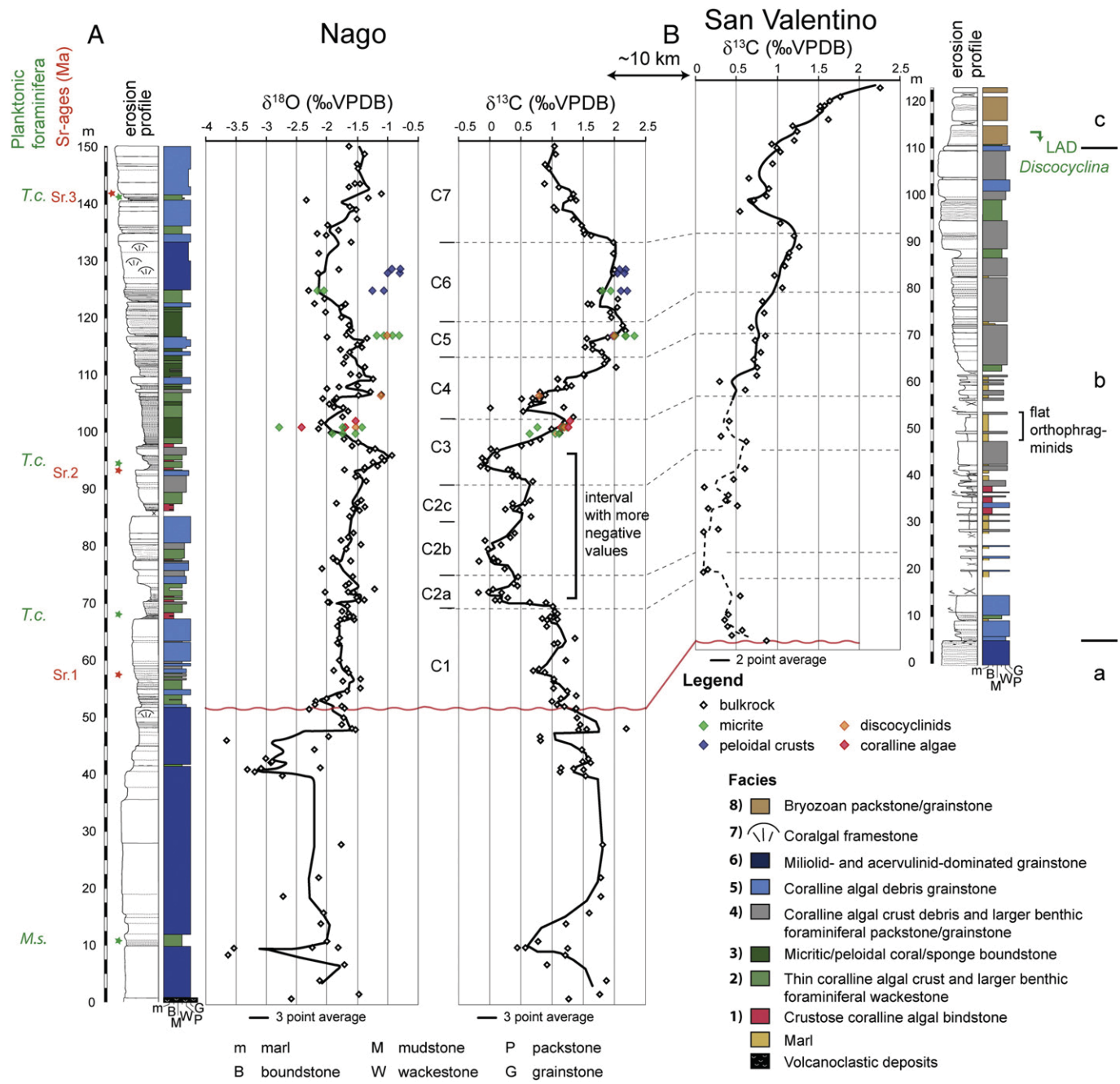

Fig. 2. A) Erosion profile and facies of the Calcare di Nago Formation in Nago together with $\delta^{18}O$ and $\delta^{13}C$ values. The carbon-isotope curve is subdivided into chemostratigraphic segments (C1–7) discussed in the text. Coloured diamonds represent the isotope values of microdrill-samples. Red stars mark the position of samples used for strontium-isotope stratigraphy. Sample positions with the planktonic foraminifera *Morozovella spinulosa* (M.s.) and *Turborotalia cunialensis* (T.c.) are indicated by green stars. Wavy red line represents the inferred hiatus. B) Erosion profile and facies of the San Valentino section and $\delta^{13}C$ curve, also showing the last appearance datum (LAD) of *Discocyclina*. a) Miliolid dominated facies (Facies 6, Table 1), b) larger benthic foraminifera and coralline-algal dominated facies (Facies 1–5), and c) bryozoan packstone/grainstone (Facies 8).

This evolution resembles that in Nago, where the lower part is referable to the Middle Eocene and the upper part to the latest Eocene. Accordingly, an important stratigraphic gap must be postulated between the lower and upper part of the section (Fig. 2).

The Calcare di Nago Formation is overlain by the Marne di Bolognano Formation. Its base is Early Oligocene in age (Luciani, 1989), belonging to the P18 zone of Blow (1979) and Berggren et al. (1995). The planktonic foraminifer *Globigerina tapuriensis* occurs within the lower part of the Marne di Bolognano (Luciani, 1989). In the Massignano section, the FAD of *G. tapuriensis* is 2 m above the Eocene–Oligocene boundary (Coccioni et al., 1988).

3. Methods

The 150 m thick succession of the Nago section was logged and sampled in detail (Fig. 2). A sequence-stratigraphic interpretation was performed based on the principles described in Strasser et al. (1999) and Catuneanu et al. (2009). Thin sections of 210 samples were made for microfacies analysis and biostratigraphy. Six marl samples were wet-sieved, and the residue was analysed under a binocular for biostratigraphic purposes.

San Valentino is a complementary section that was sampled in order to cover the last appearance datum of *Discocyclina* (Fig. 2), which is

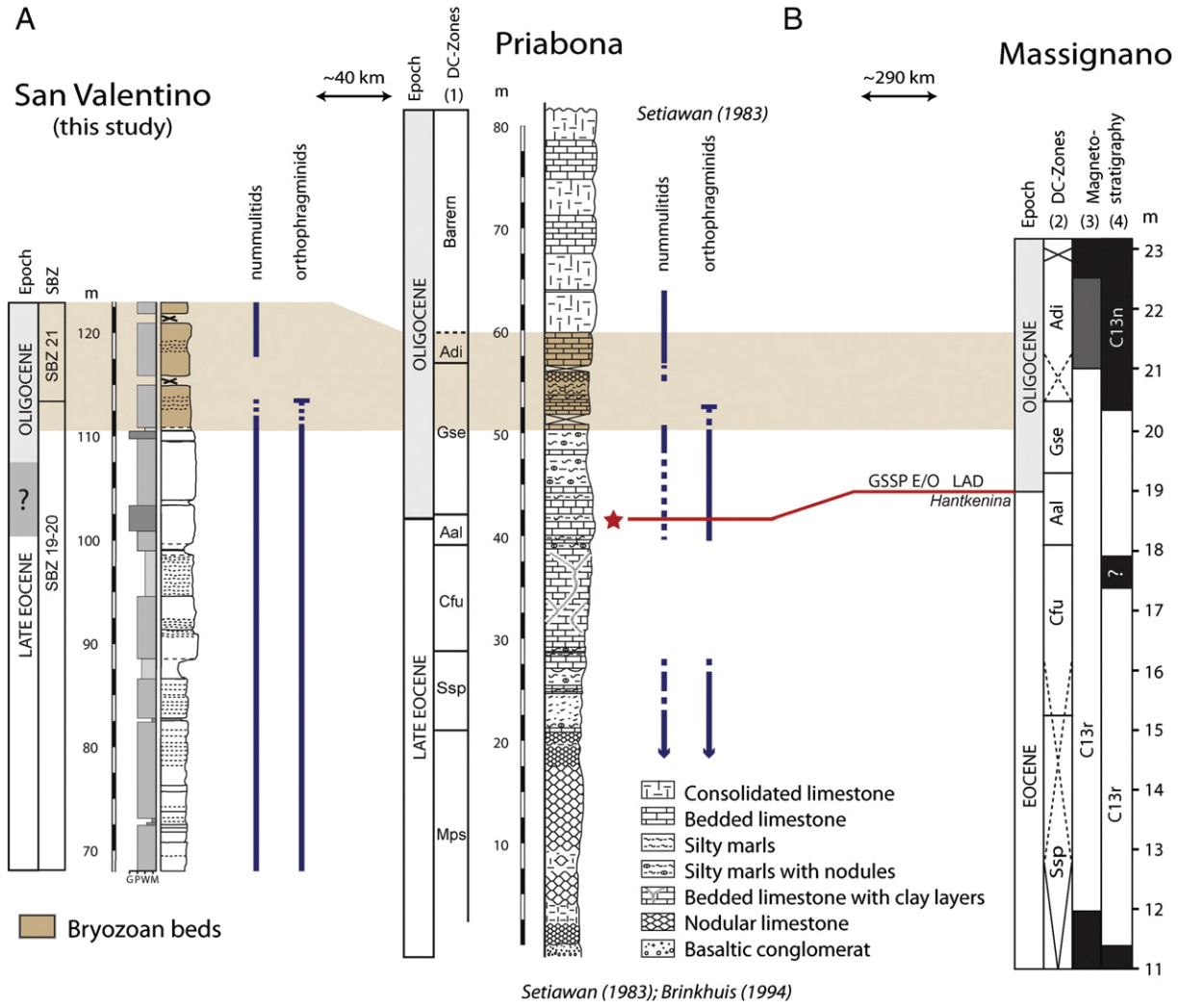

Fig. 3. A) Lithostratigraphic correlation of the bryozoan beds in the upper part of the San Valentino section and in the Priabonian type locality at Priabona (brown shaded area). Blue lines indicate the distribution of nummulitid (*Nummulites*, *Operculina*, and *Heterostegina*) and orthophragminid (*Discocyclina* and *Asterocyclina*) larger benthic foraminifera. While *Discocyclina* and *Asterocyclina* become extinct within the bryozoan beds, nummulitids (*Operculina and Nummulites*) reoccur within the upper part. Shallow benthic zonation in San Valentino (SBZ) is based on Castellarin and Cita (1969a) and Serra-Kiel et al. (1998). Dinoflagellate cyst zones in Priabona are from (1) Brinkhuis (1994). B) Massigano section displaying the dinoflagellate cyst biostratigraphic data from (2) Brinkhuis and Biffi (1993). Magnetostratigraphy is after (3) Lowrie and Lanci (1994) and (4) Bice and Montanari (1988). Red star indicates the position of the Eocene-Oligocene boundary in Priabona, as it was defined in Massignano (GSSP; Nocchi et al., 1988; Premoli Silva and Jenkins, 1993). Note that the bryozoan beds correspond to the transition between the Gse and Adi zones, which in Massignano occurs at around the base of magnetochron C13 n. (For interpretation of the references to colour in this figure legend, the reader is referred to the web of this article.)

missing in the Nago section. The lower part of the section is marly, tectonized, and partly covered. Therefore, the lower part of the section was sampled at a lower resolution (a total of 72 thin sections).

The carbon- and oxygen-isotope composition of 161 bulk samples of the Nago section and 59 of San Valentino was analysed (Fig. 2). Additionally, 27 sub-samples from different carbonate components on seven selected slabs from the Nago section were drilled and analysed in order to test the internal variability of stable isotope signatures within a single sample. Components drilled include coralline algae, discocyclinids, peloids, and micrite matrix. Isotope measurements were performed using a Finnigan MAT Delta Plus XL mass spectrometer equipped with an automated GasBench II at the Institute of Mineralogy and Geochemistry of the University of Lausanne (Switzerland). All results are reported in ‰ relative to the VPDB standard. The analytical reproducibility for three runs in Nago is better than ±0.08‰ for both $\delta^{13}C$ and $\delta^{18}O$. In San Valentino, the analytical reproducibility for three runs is better than ±0.1‰ for both $\delta^{13}C$ and $\delta^{18}O$.

For Sr-isotope stratigraphy (SIS), four oyster shells were collected from three different stratigraphic levels in the upper part of the Nago section. Samples were selected in the field and then prepared in the laboratory following the methods described in Frijia and Parente (2008) and Boix et al. (2011). The most delicate step when using SIS is to assess if the original marine Sr-isotopic signal is preserved in the samples and not altered by diagenesis. Oysters produce a primarily low-Mg calcite shell. Hence, they are more resistant to diagenetic alteration and have been proven to preserve pristine seawater Sr records in unaltered samples (DePaolo and Ingram, 1985; Jones et al., 1994; Schneider et al., 2009). In order to assess the preservation of the original shell microstructure, the samples were passed through a complete petrographic and geochemical screening by analysing the elemental (Mg, Sr, Mn, and Fe) composition of the shells. The micritic matrix of some samples was also analysed for comparison with the shells to constrain the diagenetic pathways. All geochemical analyses were performed at the Institute for Geology, Mineralogy and Geophysics of the Ruhr-University (Bochum, Germany). Concentrations of Mg, Sr, Fe, and Mn were determined through ICP-AES Thermo Fisher Scientific iCAP6500 Dual View (refer to Boix et al., 2011, for analytical procedures and reproducibility of replicate analyses).

Strontium-isotope ratios were analyzed on a Finnigan MAT 262 thermal-ionization mass spectrometer and normalized to an $^{86}Sr/^{88}Sr$ value of 0.1194.The long-term mean of modern seawater (USGS EN-1) measured at the Bochum isotope laboratory is 0.709159 ± 0.000002 (2 s.e., n = 196). The $^{87}Sr/^{86}Sr$ ratios of the samples were adjusted to the value of 0.709175 of the USGS EN-1 standard, to be consistent with the normalization used in the compilation of the look-up table of McArthur et al. (2001; version 4: 08/04), which was used to derive the preferred numerical ages of the analyzed samples and the 95% confidence limits (see Steuber, 2003, for a graphical explanation). This look-up table is tied to the Geological Time Scale of Gradstein et al. (2004).

4. Results

4.1. Sedimentary evolution of the Calcare di Nago Formation

The Calcare di Nago Formation is represented in the Nago area by a 150 m thick limestone succession overlaying volcanoclastic deposits. The first 52 m of the section (Figs. 2 and 4A) are characterized by massive beds of well-sorted miliolid- and acervulinid-dominated grainstones, occurring together with small coralgal patch-reefs in the uppermost part of this interval (photozoan association *sensu* James, 1997; Facies 6 and 7 of Table 1, Fig. 4C). These beds correspond to the lower large-scale shallowing-up cycle described by Luciani (1989). Rocks between 40 and 52 m contain components with micritic envelopes around sparry calcite cement, which implies dissolution of originally aragonitic grains in a meteoric diagenetic environment (Fig. 4C). At metre 52, an abrupt change to facies dominated by larger symbiont-bearing benthic foraminifera and non-geniculate coralline algae is observed. The larger benthic foraminifera and associated corals also imply a photozoan association. However, when compared to the miliolid- and acervulinid-dominated grainstones below, there is a decrease in abundance of primarily aragonitic components, as evidenced by less micritic envelopes. This facies change corresponds to the base of the second large-scale cycle of Luciani (1989), which is characterized by a 40 cm thick interval containing siliciclastic grains. Above, a stepwise large-scale fining of components and an increase in micrite-supported fabrics, together with a thinning of beds, is observed. This evolution is accompanied by a change in dominance of larger benthic foraminifera, passing from a nummulitid/orthophragminid- to an orthophragminid-dominated association around metre 95. Lithologically, this evolution corresponds to an upward decrease in abundance of grainstones and rudstones of the coralline algal debris facies (Facies 5). Above metre 95, the deposits are dominated by thin coralline algal crusts and larger benthic foraminiferal wackestones/floatstones (Facies 2). Micritic/peloidal coral/sponge boundstones (Facies 3) occur intercalated in Facies 2. In the upper part of the section, between metres 125 and 134, coralgal patch-reefs (Facies 7), previously described by Bosellini (1998), are present. Voids within these coralgal framestones are filled with sediment containing abundant small miliolids, dasycladaceans, and gastropods, similar to the facies found below metre 52. From 134 m upwards, thick packages of Facies 5 dominate up to the top of the section.

The evolution of the Calcare di Nago Formation in San Valentino is similar to that observed in Nago, except for the presence of more abundant marly intervals (Fig. 2). The lower part of the section directly overlaying the volcanoclastic deposits was not sampled. The measured section begins at the transition between the miliolid and geniculate red-algal grainstone to non-geniculate coralline algal and larger benthic foraminiferal limestones. Similar to Nago, rocks within this transition contain siliciclastic components. In the middle part of the section (~50 m), sediments are composed of marls and marly limestones with intercalated coralline algal bindstones and extremely flat orthophragminids (Fig. 4D,E). At metre 110, a second major facies change occurs. Red-algal and larger benthic foraminiferal limestones (photozoan association, Fig. 4F) are replaced by bryozoan-dominated grainstones/packstones (heterozoan association sensu James, 1997; Facies 8, Fig. 4G).

4.2. Carbon and oxygen isotopes in Nago and San Valentino

Carbon and oxygen stable isotopes were measured throughout the Nago section (Fig. 2). However, only the Late Eocene interval (above 52 m) is taken into account because biostratigraphic data suggest the presence of a hiatus of uncertain duration around metre 52. The $\delta^{13}C$ curve can be subdivided into 8 chemostratigraphic segments (Fig. 2). Chemostratigraphic segment-boundaries are defined by turning points from positive to negative shifts.

The lowermost interval (segment C1) starts around metre 53. It is characterized by a negative shift displaying an amplitude of around 0.5‰, leading to a small spike at metre 57. Above this peak, there is a return to pre-shift values (mean + 1.00‰). Segment C2 is characterized at its base by a pronounced negative shift of 1.12‰, starting at around metre 70 and marking the base of a 25 m thick interval characterized by lighter $\delta^{13}C$ values (Fig. 2). Segment C2 can be subdivided into three sub-segments. Sub-segment C2a is characterized at its base by the negative shift leading to a peak of −0.24‰ at 72.3 m. This is followed by a rise of the values to +0.42‰. At the base of segment C2b, the curve displays a decrease to −0.22‰ at 77.7 m, followed by a gradual positive shift reaching a value of +0.66‰. Within this positive shift, segment C2c is characterized by a small negative spike with an amplitude of 0.4‰.

A prominent negative shift of ~1‰ characterizes the lower part of C3, where $\delta^{13}C$ values of −0.20‰ are reached, corresponding to the last portion of the 25 m thick negative interval (Fig. 2). From this point, a stepwise shift (~95 to 120 m) to more positive values occurs. This shift is interrupted by a negative spike, defining segment C4. A small spike at the end of the positive trend characterizes segment C5. Segment C6 is defined at the base by the most positive values recorded in Nago (+2.19‰), followed by a rapid but low-amplitude (0.62‰) negative shift. The positive shift recorded above this peak displays a gentle slope leading to stable values (~2.0‰), making a plateau that persists for more than 10 m.

Segment C7 is characterized by a renewed negative $\delta^{13}C$ shift with an amplitude of ~1.00‰, followed by a plateau at around +1.00‰ up to the top of the Nago section.

Due to the poor outcrop conditions in the lower part of the San Valentino section and the resulting lower sampling resolution, the recognition of individual chemostratigraphic segments is more difficult. However, a negative shift in $\delta^{13}C$ similar to the one recorded in Nago marking the beginning of C1 occurs below metre 10. This is followed

Fig. 4. (A) Picture of the Calcare di Nago Formation outcropping north of Nago. White line indicates the position of the inferred hiatus at metre 52 and the transition between well-sorted miliolid-dominated grainstones to larger benthic foraminifera and coralline-algal dominated facies. (B) Outcrop of the Calcare di Nago Formation (CNFm) northwest of San Valentino. The transition between larger benthic foraminiferal and coralline-algal dominated facies (b, photozoan association) to bryozoan packstone/grainstone (c, heterozoan association) is represented by a white line. (C) Photomicrograph of a miliolid-dominated limestone (photozoan association, Facies 6). Although originally aragonitic components (mainly green algae, coral fragments and bivalves) have been dissolved, their shape is preserved due to micritic envelopes. Magnification (bottom left) shows interparticle and moldic porosity filled with sparry cement (Nago, 49 m). (D) and (E) Polished slab and photomicrograph of a limestone dominated by thin orthophragminids (*Discocyclina* and *Asterocyclina*) and thin red-algal crusts. Matrix between the components is a wackestone (San Valentino, 52 m). (F) Photomicrograph showing a red-algal and larger benthic foraminiferal packstone (photozoan association, Facies 5), sampled at metre 110 in San Valentino. (G) Bryozoan packstone representing a heterozoan association (San Valentino, 116 m). Matrix is mainly composed of fine bryozoan and echinoderm debris (Facies 8). (For interpretation of the references to colour in this figure legend, the reader is referred to the web of this article.)

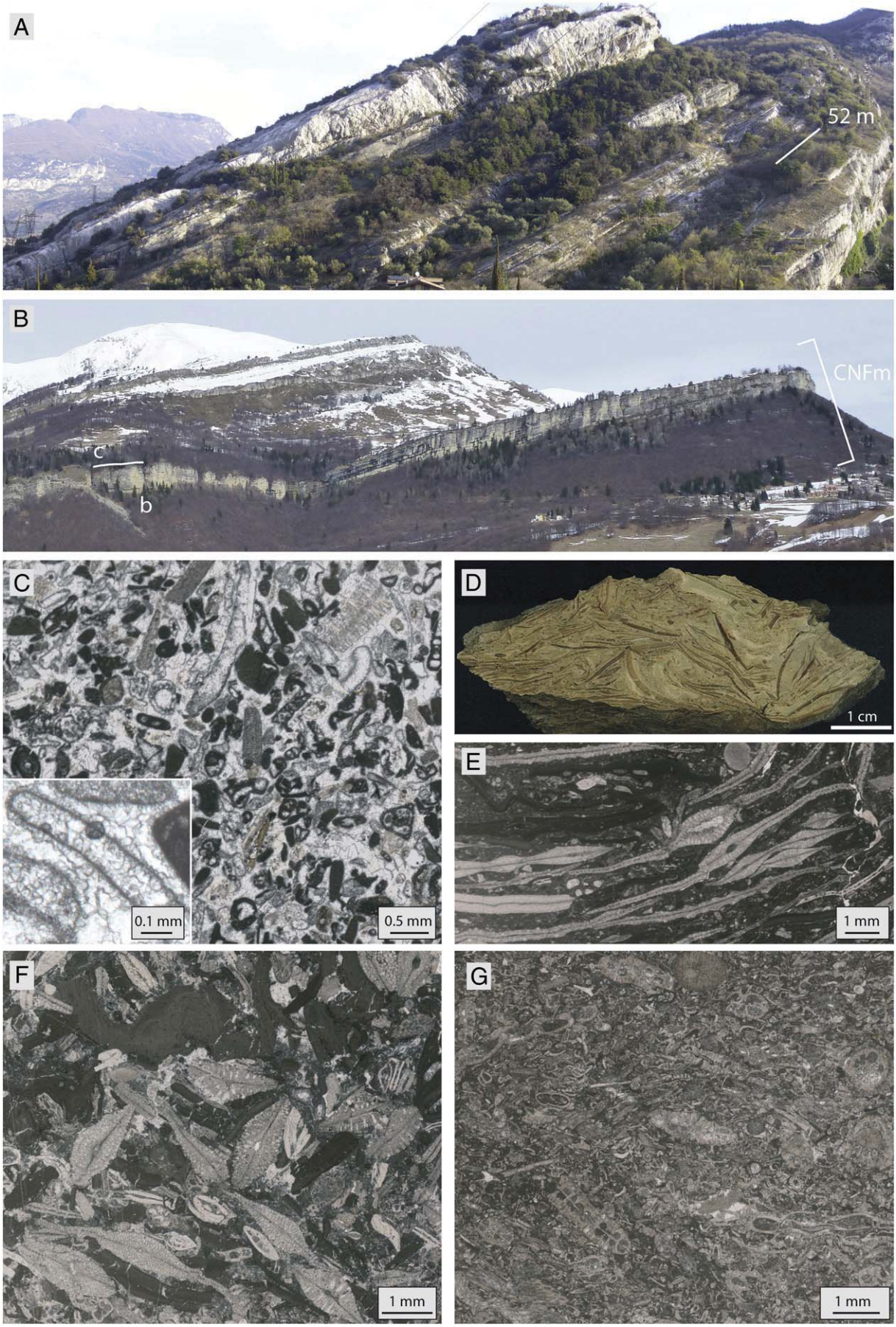

Table 1
Description and interpretation of the lithofacies recognized in this study.

Nr.	Facies	Appearance in the field/fabric	Main constituents	Depositional environment
8	Bryozoan packstone/ grainstone	Massive beds/highly bioturbated, components moderately well sorted	Bryozoan debris (up to 90%), echinoderms, non-geniculate red algae, agglutinated and planktonic foraminifera. In the lower part few broken nummulitid and discocyclinid foraminifera filled with glauconite are present. In the upper part nummulitids reoccur.	High energy, middle to outer ramp
7	Coralgal framestone	Massive limestones	Corals (*Actinasis rollei* showing laminar and platy growth-forms and *Plocophyllia bartai* with phaceloid and massive growth forms; Bosellini, 1998), thick coralline crusts dominated by members of the Mastophoroideae subfamily (Bassi, 1998). Sediments filling voids within the framestone are attributable to the mililid-dominated grainstone facies.	High energy inner to proximal middle ramp
6	Miliolid dominated grainstone	Massive limestones/fine-grained, rounded, and well sorted grains	Small miliolids, *Borelis*, *Orbitolites*, asterigerinids, *Gypsina moussaviani*, *Chapmania*, *Halkyardia*, *Fabiania*, geniculate and non-geniculate coralline algal debris, phaceloid corals, echinoderm debris, rare *Nummulites* and discocyclinids.	High energy, shallow inner ramp.
5	Coralline algal debris grainstone	Massive/highly bioturbated, components sub-rounded to rounded, moderately- to well-sorted	Abraded non-geniculate red-algal debris and geniculate coralline algae, asterigerinids, small rotaliids, lense shaped *Nummulites* and *Discocyclina*. Less abundant are *Spiroclypeus*, *Heterostegina*, *Assilina alpina*, *Pellatispira maderazi* and *Asterocyclina*.	High energy, inner to middle ramp
4	Coralline algal crust debris and larger benthic foraminiferal packstone/grainstone	Massive/highly bioturbated, components angular, moderately- to very poorly-sorted	Thin red algal crust debris, rhodoliths, bryozoans, *Discocyclina*, *Asterocyclina*, *Pellatispira*, *Biplanispira*, *Heterostegina*, *Assilina alpina*, *Spiroclypeus* and *Nummulites*.	Moderate to low energy, middle to outer ramp
3	Micritic/peloidal coral/sponge boundstone	Wavy-bedded/highly bioturbated, bioconstructed framework with wackestone matrix	Thin coralline algal crusts (melobesioid dominated association, Bassi, 1998), solitary and thin laminar corals (*Actinacis rollei-Cyathoseris* association, Bosellini, 1998), sponge spicules, orthophragminids (*Discocyclina* and *Asterocyclina*), planktonic foraminifera, and peloids.	Low energy, outer ramp
2	Thin coralline algal crust and larger benthic foraminiferal wackestone/floatstone	Wavy-bedded limestones with marly intercalations/highly bioturbated, up to 10 cm thick tempestite layers intercalated	Thin coralline crusts (melobesioid-dominated association), orthophragminids (*Discocyclina* and *Asterocyclina*), bryozoans, planktonic foraminifera. Although less abundant, nummulitid foraminifera (*Spiroclypeus*, *Heterostegina*, *Assilina alpina*, *Pellatispira maderazi*) can be present.	Low energy, outer ramp
1	Crustose coralline algal bindstone	Wavy-bedded limestones and marly limestones/bindstone constructed by an open framework of thin coralline crusts	Thin coralline algal crusts (melobesioid-dominated association). Packstone to wackestone matrix contains larger foraminifera (*Discocyclina, Asterocyclina, Assilina alpina, Spirocypeus)* and bryozoans. Facies associated to sub-ellipsoidal and sub-discoidal rhodoliths (6 and 8 cm) with loosely packed laminar algal thalli with a high percentage of constructional voids (60–63%; Bassi, 1998).	Low energy, outer ramp

by a more prominent negative shift characterizing the base of segment C2a. Between metres 50 and 80 (C3–C5), a long-term positive trend comparable to the one in Nago (between 95 and 120 m) is recorded. In San Valentino, the upper part of C6 does not show an interval with constant values as in Nago but a relatively sharp positive spike. However, above this spike, the base of segment C7 is characterized by a prominent negative shift, as in Nago. In San Valentino, which additionally contains younger rocks than Nago, the plateau characterizing the upper part of segment C7 is followed by a prominent positive shift reaching the most positive values (+2.24‰).

The stable carbon isotopes in San Valentino thus display a long-term pattern similar to the one recognized in Nago (Fig. 2), although the amplitudes are lower.

4.3. Strontium isotope stratigraphy and numerical ages

The first sample analyzed (Sr. 1, Table 2) comes from a bed containing red-algal and larger benthic foraminiferal grainstones of Facies 5 (58 m). The $^{87}Sr/^{86}Sr$ ratio of 0.707790 translates into a numerical age of 34.39 Ma (+/−0.76–0.4), corresponding to the latest Eocene (latest Priabonian). The second dated level at 93 m (Sr. 2, Table 2) was sampled within an interval containing grainstones of Facies 5. It corresponds to a level occurring in the lower part of segment C3 of the carbon isotope curve. The Sr-isotopic value of 0.707800 gives a numerical age of 34.14 Ma (+/−0.64–0.39), again corresponding to the latest Eocene. The third dated level (Sr. 3, Table 2) occurs at 142 m within a grainstone of Facies 5, within segment C7 of the carbon isotope curve. The value of 0.707802 translates into an age of 34.09 Ma (+/−0.59–0.37), corresponding to the latest Eocene, very close to the Eocene–Oligocene boundary placed at 33.9 Ma by Gradstein et al. (2004).

5. Discussion

5.1. Carbon-isotope values

The use of carbon-isotope chemostratigraphy has become a powerful tool for chronostratigraphic correlations between platform and pelagic sections (Jenkyns, 1995; Vahrenkamp, 1996; Ferreri et al., 1997; Grötsch et al., 1998; Menegatti et al., 1998; Stoll and Schrag, 2000; Mutti et al., 2006; Parente et al., 2007; Burla et al., 2008; Huck et al., 2011). Limitations result mainly from diagenetic alteration (Hudson, 1977; Dickson and Coleman, 1980; Brand and Veizer, 1981; Veizer, 1983; Marshall, 1992), aging of water masses within restricted environments (Immenhauser et al., 2002), and changing proportions of aragonite vs. low-magnesium calcite within the rocks, as aragonite is naturally enriched in $\delta^{13}C$ if compared to calcite precipitated from the same fluid (Swart, 2008).

Sediments in Nago and San Valentino were deposited in open-marine conditions. Therefore, it is believed that no important aging of water masses occurred. The vertical facies evolution in both sections is highly heterogeneous, containing intervals with different proportions of primary aragonitic components (corals), but no correlation between facies and stable isotope trends is observed (Fig. 2). The low covariance ($R^2 = 0.0889$ in Nago and $R^2 = 0.0848$ in San Valentino) between the carbon and the oxygen isotopes in the sections (Fig. 5) can be interpreted as indicating negligible diagenetic overprint (Menegatti et al., 1998; Burla et al., 2008). Therefore, it is interpreted that the

Table 2
Strontium-isotope stratigraphy of the Nago section. P = pristine; A = altered; na = not available. Numerical ages are derived from McArthur et al. (2001; look-up table version 4: 08/04). The precision of the $^{87}Sr/^{86}Sr$ mean value for each stratigraphic level is given as 2 s.e. of the mean and considered to be not better than the average precision of single measurements (2 s.e. = 0.000007). It is calculated from the standard deviation of the mean value of the standards run with the samples (n = 1, 0.000012; n = 2, 0.000009).

Sample	Level	Section	Material	Ca (ppm)	Sr (ppm)	Mg (ppm)	Fe (ppm)	Mn (ppm)	$^{87}Sr/^{86}Sr$ measured	2 s.e ($*10^{-6}$)	$^{87}Sr/^{86}Sr$	Alteration	$^{87}Sr/^{86}Sr$ mean	2 s.e. mean ($*10^{-6}$)	min	Age (Ma) preferred	max
CN-3B	**Sr. 1**	Nago	ostreid	390720	716	1905	140	5	0.707771	0.000006	0.707787	P					
CN-3A		Nago	ostreid	na	na	na	na	na	0.707777	0.000007	0.707793	P					
mean													0.707790	9	33.99	**34.39**	35.15
CN-1A	**Sr. 2**	Nago	ostreid	395330	640	1157	115	4	0.707784	0.000006	0.707800	P	0.707800	12	33.75	**34.14**	34.78
CN-4A	**Sr. 3**	Nago	ostreid	394830	581	1878	108	19	0.707786	0.000007	0.707802	P	0.707802	12	33.72	**34.09**	34.68
CN-4 M		Nago	matrix	389870	307	4061	260	33	0.707851	0.000006	0.707867						

$\delta^{13}C$ evolution in Nago and in the upper part of San Valentino follows, at least partly, global trends.

Negative $\delta^{18}O$ values below metre 52 in Nago (Figs. 2 and 5), ranging between −2.5 and −4‰, are interpreted to be due to diagenetic alteration, which probably took place during short periods of subaerial exposure.

Carbon-isotope values of microdrilled single components measured in Nago plot very close to the respective values obtained from bulk analyses (Fig. 2), supporting the idea that bulk values match the marine isotopic record. In contrast to $\delta^{13}C$ values, $\delta^{18}O$ values are more scattered.

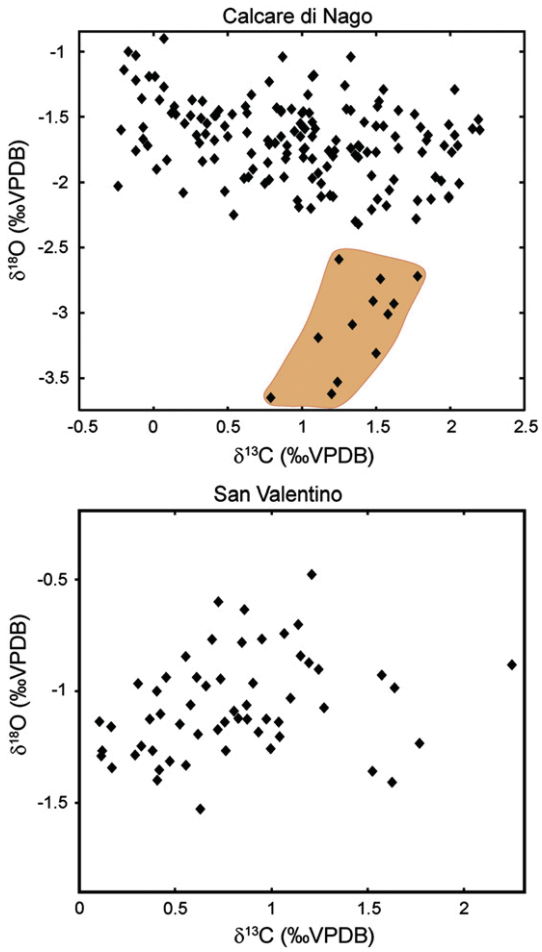

Fig. 5. Cross-plots of $\delta^{13}C$ and $\delta^{18}O$ values from carbonate bulk rock samples of the Nago and San Valentino sections. Note the low covariance between $\delta^{13}C$ and $\delta^{18}O$ indicating the absence of strong diagenetic alteration. Values within the orange-shaded area of the Nago plot were measured metre 52 (Fig. 2). (For interpretation of the references to colour in this figure legend, the reader is referred to the web of this article.)

5.2. Strontium isotope stratigraphy

The age of the upper part of Nago section has been constrained by means of Sr-isotope stratigraphy (SIS), a powerful tool for dating and correlating shallow-marine carbonate deposits (Steuber et al., 2005, 2007; Frijia and Parente, 2008; Boix et al., 2011).

Trace element analysis of the oyster samples (Table 2) reveal Mg concentrations in the range of low-Mg calcite shells and Sr concentrations in the range of extant and well-preserved fossils oysters (Schneider et al., 2009). The Mn concentrations for all samples are below the 50 ppm cut-off limit of Jones et al. (1994) for well-preserved ostreids.

Trace element values of the shells contrast with those of the matrix, which yields much higher concentrations of Fe, Mg, and Mn associated with lower Sr (Table 2). Furthermore the $^{87}Sr/^{86}Sr$ ratio of the matrix is more radiogenic than in oysters from the same level, suggesting that the diagenetic fluids had a higher $^{87}Sr/^{86}Sr$ signal than the original seawater.

Finally, the pattern of changes of $^{87}Sr/^{86}Sr$ throughout the section and the consistency of the Sr isotope composition within an individual stratigraphic level (Sr.1, Table 2) argues against diagenetic alteration, which may otherwise lead to unsystematic changes in the Sr isotope composition (McArthur, 1994; McArthur et al., 2004; Steuber et al., 2005; Frijia and Parente, 2008). Consequently, it is considered that all our samples preserve their pristine $^{87}Sr/^{86}Sr$ composition.

5.3. Platform-to-basin correlation

The closely spaced Nago and San Valentino sections can be correlated by bio-, chemo-, and lithostratigraphy, supporting a coeval evolution of both successions. Concerning the carbon isotopes, the most complete deep-sea records show that the latest Eocene is characterized by a shift to more negative values (Poag et al., 2003) prior to the positive shift defining the EOT (Fig. 6). This is well recognized within the $\delta^{13}C$ curves of Massignano, ODP Site 744, and TDP Sites 12 and 17, where a period of 0.5 to 1 myr of relatively stable values is followed by an interval of more unstable values, showing several negative excursions.

The here proposed correlation between our platform sections and pelagic records has been achieved using biostratigraphic data together with strontium isotope ages as tie points to anchor the $\delta^{13}C$ curves, so that key peaks and inflection points of these curves can be used for a high-resolution correlation (Fig. 6).

Probably the most important tie-point allowing a chemostratigraphic correlation corresponds to the extinctions of *Discocyclina* and *Asterocyclina* within the bryozoan beds in San Valentino. The combination of these events allows an unequivocal correlation to the Priabona area (Fig. 3), where they occur around the transition between the Gse and Adi dinoflagellate cyst zones (Brinkhuis, 1994).

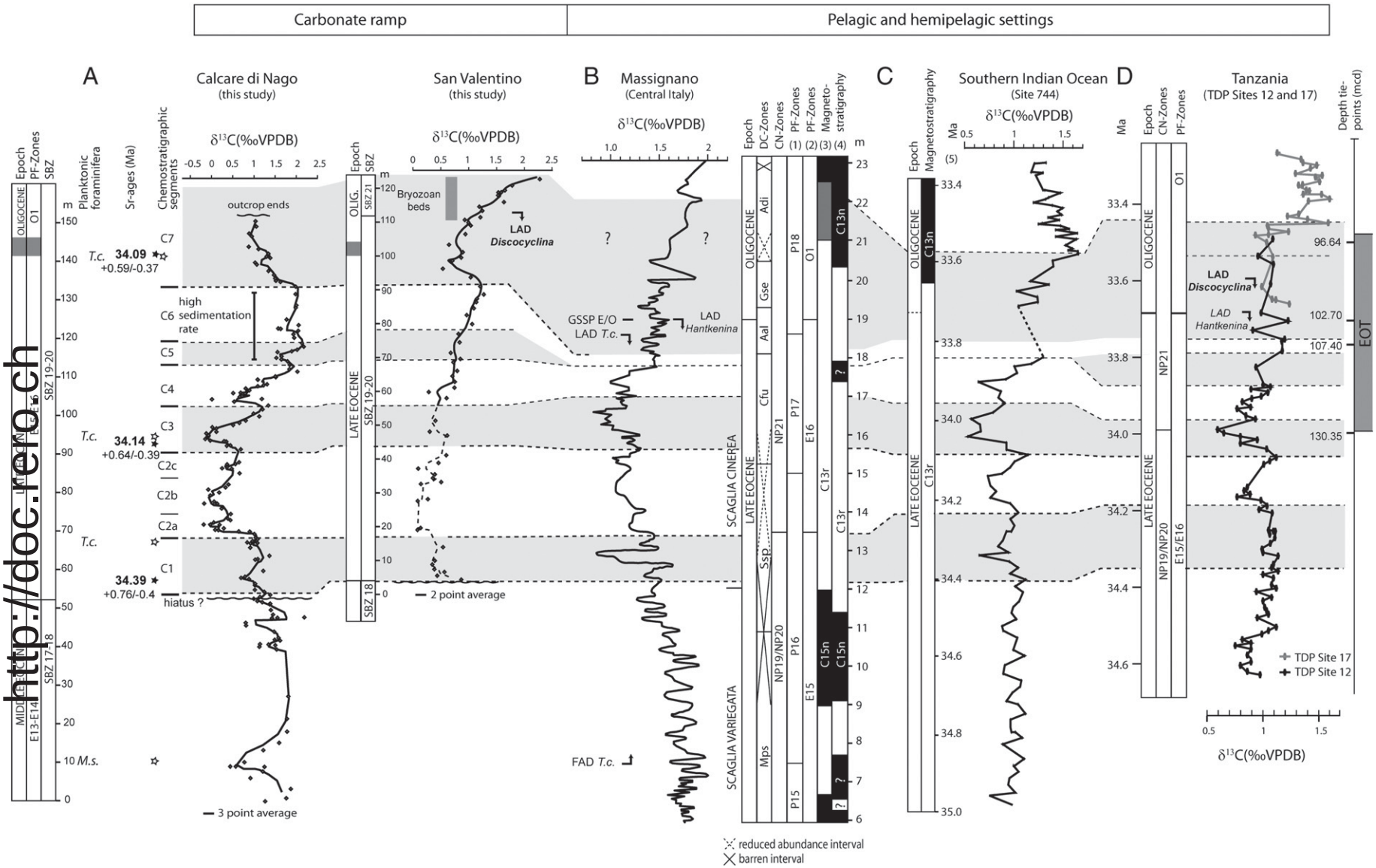

Fig. 6. Tentative chemostratigraphic correlation between the studied shallow-water successions and three deep-water sections in the Tethys realm, the southern Indian Ocean, and Tanzania. A) Bulk rock stable carbon-isotope curves of the Nago and San Valentino sections with chemostratigraphic segments. Black stars mark the position of Sr-samples. Numerical ages derived from strontium isotope stratigraphy are tied to the chronostratigraphic chart of Gradstein et al. (2004) where the Eocene–Oligocene boundary is placed at 33.9 Ma. The occurrence of *Morozovella spinulosa (M.s.)*, *Turborotalia cunialensis* (*T.c.*) (white stars), and last appearance datum (LAD) of *Discocyclina* are shown. Planktonic foraminifera (PF) zones follow Berggren and Pearson (2005), shallow benthic zones (SBZ) Serra-Kiel et al. (1998). B) Carbon-isotope curve of the Massignano section measured on bulk rock (Bodiselitsch et al., 2004; Brown et al., 2009), displaying the position of the Global Stratotype Section and Point (GSSP) defined by LAD of *Hantkenina* at metre 19 (Nocchi et al., 1988; Premoli Silva and Jenkins, 1993). Also shown is the range of *Turborotalia cunialensis (T.c.)* after Coccioni et al. (1988). Dinoflagellate cysts (DC) after Brinkhuis and Biffi (1993); Calcareous nannoplankton (CN) zones after Martini (1971); PF zones after (1) Berggren et al. (1995) and (2) Berggren and Pearson (2005). Magnetostratigraphy is after (3) Lowrie and Lanci (1994) and (4) Bice and Montanari (1988). C) Stable carbon-isotope curve of ODP Site 744 measured on benthic foraminifera (*Cibicidoides* spp., Zachos et al., 1996). Dashed part of the curve corresponds to a 50 cm thick interval which was not sampled because of severe drilling disturbance. Age model (5) is based on conversion to Site 1218 (Coxall and Wilson, 2011). D) Composite carbon-isotope curve of TDP Sites 12 and 17 (measured on planktonic foraminifera *Turborotalia ampliapertura*) plotted against CN and PF zones and the LAD of *Hantkenina* (Pearson et al., 2008). LAD of *Discocyclina* is based on Cotton and Pearson (2011). Numerical ages are according to Berggren et al. (1995) and Berggren and Pearson (2005), placing the Eocene–Oligocene boundary at 33.7 Ma.

At Massignano the transition from the Gse to the Adi zone is found around metre 21 (Brinkhuis and Biffi, 1993), roughly coinciding with the base of magnetochron C 13 n, which further permits a correlation to ODP Site 744 where magnetostratigraphic data are available (Fig. 6).

Numerical ages derived from strontium isotope stratigraphy are not absolute ages but are derived from a look-up table tied to the Geological Time Scale of Gradstein et al. (2004) (see methods chapter), which places the Eocene–Oligocene boundary at 33.9 Ma. Therefore, the numerical ages in Nago are not directly comparable to the ones in the pelagic sections presented in Fig. 6 where the Eocene–Oligocene boundary is dated at 33.7 Ma according the time scale of Berggren et al. (1995) and Berggren and Pearson (2005). However, taking into account the different ages of the Eocene-Oligocene boundary depending on the timescale used and the error margins of the "preferred age" obtained with SIS (Table 2), the upper interval of the Nago section can be confidently constrained to the latest Eocene and the EOT.

Comparison of the $\delta^{13}C$ profiles at Nago and San Valentino with the curves of the deep-sea sites shows a remarkable similarity in the pattern of isotopic fluctuations. Key features used for the correlation include a prominent negative peak (chemostratigraphic segment C3), occurring in the uppermost part of the negative interval (C2a–C3). Following this peak, a prolonged positive shift superimposed by a negative spike corresponding to segment C4 is recognized in all localities. Another key feature to correlate the shallow and basinal sections is a negative shift occurring at the base of C7 followed by a short plateau and a prominent prositive shift characterizing the upper part of segment C7 (the positive shift is missing in Nago because the outcrop ends exactly where it would be expected).

The LAD of *Discocyclina* and other larger benthic foraminifera including a number of species of *Nummulites* in Tanzania occurs between 102.14 and 99.55 mcd, shortly postdating the Eocene/Oligocene boundary at 102.28 mcd (Cotton and Pearson, 2011). Although in San Valentino the LAD of *Discocyclina* appears to be somewhat later than the extinction of the genus in Tanzania, it occurs in segment C7 at a similar position relative to the carbon curve, providing additional support for the proposed correlation.

According to bio- and magnetostratigraphy, the Massignano section was deposited coevally with the other sections. However, the correlation of the $\delta^{13}C$ curve is not straightforward, most probably due to a moderate diagenetic overprint (Coccioni et al., 2000; Vonhof et al., 2000; Bodiselitsch et al., 2004) and/or to locally different oceanographic conditions.

Below metre 13, a prominent negative shift is recorded in Massignano. In Nago, San Valentino, and Tanzania, only a relatively small peak is seen at this position.

A prominent positive carbon-isotope shift has been globally recognized (e.g., in ODP Sites 744 and 1218 and in DSDP Site 522), just above the base of magnetochron C13n. This shift is not clearly developed in Massignano. The positive shift recorded at metre 20 is produced by only one value (Bodiselitsch et al., 2004), which is below the base of C13n. Therefore, it does not correspond to the above mentioned positive shift.

Segment C6 in Nago is represented by a thick (15 m) interval with relatively constant positive $\delta^{13}C$ values. The corresponding intervals in TDP Sites 12 and 17 and Massignano do not show this pattern of prolonged constant values. Within the Nago section, this interval corresponds mostly to a coralgal framestone, interpreted to have been deposited at a higher sedimentation rate compared to the rest of the deposits. Therefore, it is likely to represent a local phenomenon.

The carbon-isotope records of the Nago and San Valentino sections show shifts with higher amplitudes than the coeval pelagic records. Similar observations have been made by other researchers who have reported higher amplitudes in shallow-marine sections when compared to pelagic ones (Jenkyns, 1995; Vahrenkamp, 1996; Grötsch et al., 1998; Wissler et al., 2003; Burla et al., 2008; Huck et al., 2011). This has been explained by arguing that shallow waters are less stable in their isotopic composition and more sensitive to a variety of factors including local changes in productivity or organic matter reservoirs that may amplify open oceanic patterns in $\delta^{13}C$.

Although debated, the most common explanation for the globally recognized positive excursion of carbon isotopes around the Oi-1, found also in the upper part of segment C7 in the shallow-marine San Valentino section, is a global increase in export and burial of organic carbon in the deep-sea (Salamy and Zachos, 1999; Coxall and Pearson, 2007; Miller et al., 2009; Coxall and Wilson, 2011).

5.4. Record of the Late Eocene and the EOT sea-level and climate changes in the Calcare di Nago Formation

The platform-to-basin correlation proposed in this study makes it possible to compare palaeoecological and stratigraphic observations made in a shallow-marine depositional system with oceanographic events recorded in the deep-sea realm (Fig. 7).

Based on the changes in relative water depth of deposition as inferred from the facies analysis, a large-scale sequence-stratigraphic analysis of the Nago and San Valentino succession was performed. Large-scale shallowing-deepening trends are interpreted as transgressive-regressive sequences *sensu* Embry (1993).

Below metre 52 the facies succession is monotonous and dominated by thick, massive packages of shallow-water grainstones of Facies 6 and coral framestones. Based on facies evolution, no large-scale shallowing or deepening trend can be recognized. However, meteoric cements occur in the uppermost 10 m of this interval. Therefore, it can be postulated that at least the upper part represents a shallowing-up. The widespread meteoric cementation occuring within rocks composed of Facies 6 directly overlain by deposits dominated by larger benthic foraminifera and non-geniculate coralline algae (Figs. 2 and 7 and Table 1) implies a marine transgression onto an interval characterized by episodes of subaerial exposure. A similar change in facies is recorded in San Valentino. Therefore, the surface displaying this facies change is interpreted as a transgressive surface superimposed on a sequence boundary. The episodes of subaerial exposure postulated here are interpreted to be related to the regressive phase recognized on top of Bartonian deposits in the western Colli Berici (Ungaro and Bosellini, 1965; Ungaro, 1969) and the Lessini Shelf (Frascari, 1963), where it favoured the establishment of brackish conditions and, in some cases, ended with emersion. Therefore, as proposed by Papazzoni and Sirotti (1995), the transgression recorded in Nago and San Valentino is interpreted to represent the so-called Priabonian transgression (Frascari, 1963).

A 0.4‰ negative shift in the oxygen-isotope values at ODP Site 744 (Fig. 7) correlates with segment C1 in Nago. Interestingly, this negative shift coincides with the onset of the Priabonian transgression in Nago and San Valentino. As no major phase in Alpine tectonics is thought to have occurred at this time in the Southern Alps (Doglioni and Bosellini, 1987), it is postulated that the transgression was associated to a glacio-eustatic sea-level rise. It represents therefore additional evidence for the existence of at least medium-scale continental ice sheets before the beginning of the Eocene–Oligocene transition.

Variations of 0.4‰ would translate into ca. 40 m of sea-level change, following the Late Pleistocene $\delta^{18}O$/sea-level calibration (0.11‰/10 m) of Fairbanks and Matthews (1978). However, Miller et al. (2005b) stress that the average isotopic composition of past ice sheets is unknown, and that ice sheets during greenhouse intervals must have had higher $\delta^{18}O$ values than in Late Pleistocene time. Melting of ice sheets with higher $\delta^{18}O$ values has less influence on the mean ocean $\delta^{18}O$ value per unit sea-level change than melting of ice with lower $\delta^{18}O$ values (Miller et al., 2005b). Thus, the $\delta^{18}O$ fluctuation observed at ODP Site 744 could account for a sea-level rise with an amplitude even higher than 40 m.

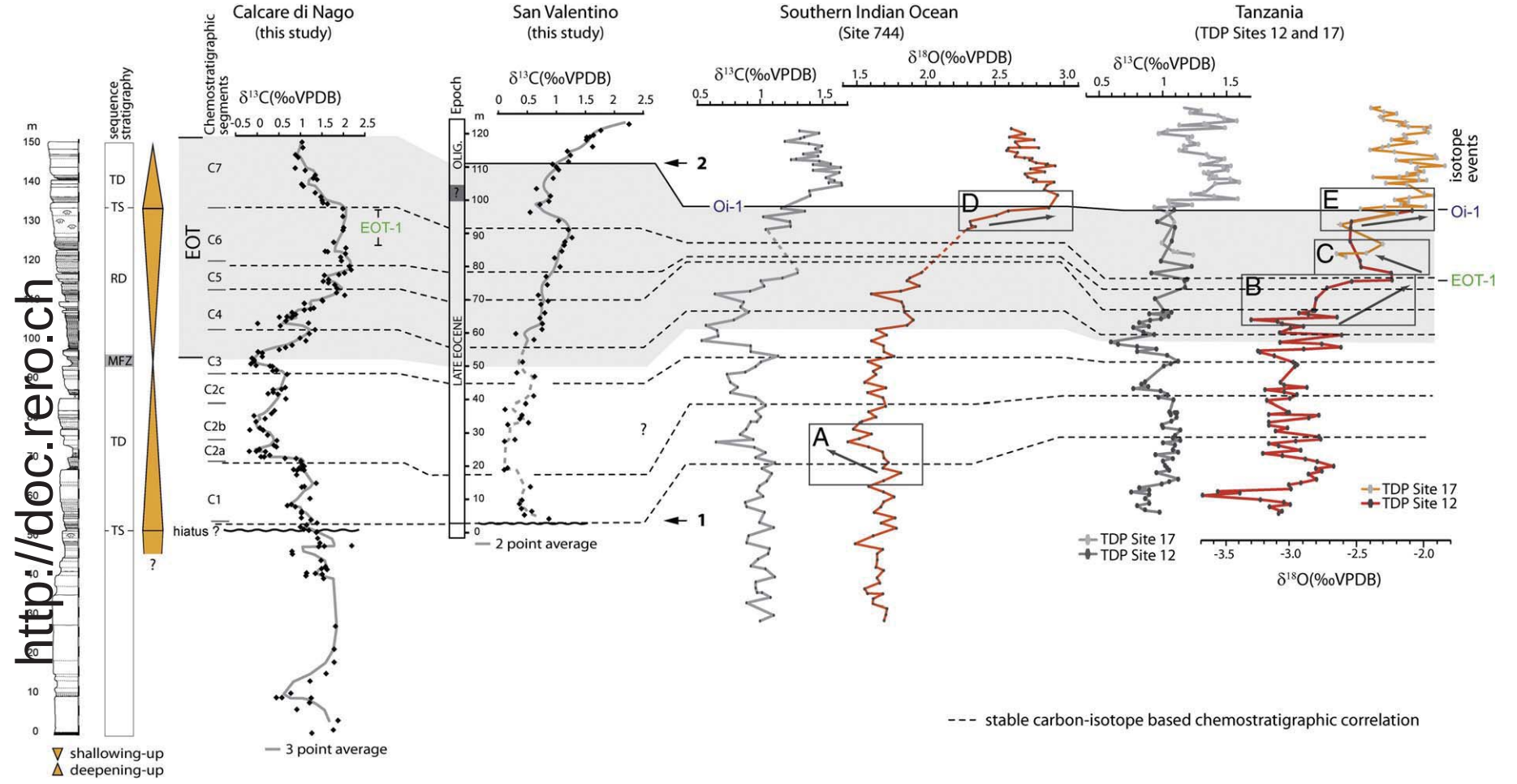

Fig. 7. Oxygen-isotope curves of ODP Site 744 (measured on *Cibicidoides* spp.) and composite TDP Sites 12 and 17 (measured on *Turboratalia ampliapertura*) showing the range of the EOT and the position of the EOT-1 and Oi-1 events, plotted against the sequence-stratigraphic and lithostratigraphic evolution in the shallow-marine Nago and San Valentino sections. Correlation and comparison is based on carbon-isotope chemostratigraphy (dashed lines, Fig. 6). Sequence-stratigraphical elements are: transgressive surface (TS), transgressive deposits (TD), maximum-flooding zone (MFZ) and regressive deposits (RD). Arrows indicate large-scale facies changes within the sections: (1) miliolid grainstone to larger benthic foraminifera and coralline algal dominated facies (Priabonian transgression in Nago and San Valentino), (2) larger benthic foraminifera and coralline-algal dominated facies (photozoan association) to bryozoan packstone/grainstone (heterozoan association) in San Valentino. Box A: negative $\delta^{18}O$ shift occurring together with a transgression in Nago and San Valentino. Box B: positive $\delta^{18}O$ shift related to the EOT-1 event in Tanzania. Box C: negative $\delta^{18}O$ shift between the EOT-1 and Oi-1 events implying warming and sea-level rise, and leading to transgressive deposits in Nago and San Valentino. Boxes D and E: positive $\delta^{18}O$ shifts resulting in the Oi-1 isotope event in ODP Site 744 and Tanzania, respectively.

Between metres 52 and 95 in the Nago section there is a stepwise decrease in dominance of thick packages of grainstones and rudstones of Facies 5, leading to a thick interval dominated by wackestones and boundstones of Facies 2 and 3. This stepwise change, responding to a decrease in energy of the depositional environment, is interpreted to be the expression of a long-term deepening. This is supported by the change in larger benthic foraminiferal assemblages, passing from a nummulitid- and orthophragminid- to orthophragminid-dominated association (Hottinger, 1997). The deepest interval marking the maximum-flooding zone (MFZ) is found around 95 m in Nago. In San Valentino, the MFZ is represented by a marly interval (around metre 50) characterized by loose bindstones constructed by thin red-algal crusts (<1 mm thick) and the dominance of very flat orthophragminids (Figs. 2 and 4D,E). Studies dealing with recent and fossil symbiont-bearing foraminifera have noted inter- and intra-specific changes in test morphology towards a thinning of chamber walls and a decreasing test sphericity (i.e. flattening) with increasing water depth (Hallock, 1979; Hallock and Glenn, 1986; Hottinger, 1997; Beavington-Penney and Racey, 2004; Cosovic et al., 2004), supporting a low energy, relatively deep environment of deposition in San Valentino.

The interval above the MFZ, representing the regressive deposits, is characterized by a stepwise shallowing of the environment ending with the establishment of massive coralgal framestones between metres 125 and 134 in Nago (Facies 7, Table 1). Smaller coral communities involved in the construction of boundstones are found throughout the Nago section within Facies 2 and 3. However, they differ in taxonomic composition, growth forms, and percentage and proportion within the framework (Bosellini, 1998), as well as in their matrix, which suggests deeper environments of formation. The coralgal framestones between metres 125 and 134 are interpreted represent the shallowest facies within the Priabonian part of the Nago section. Sediments filling voids in the coralgal frameworks contain abundant small miliolids, dasycladaceans, and gastropods (Facies 6), which suggest a shallow depositional environment. It is here interpreted that the coralgal frameworks could grow because falling sea level placed the depositional environment within the inner and most proximal middle ramp. Therefore, they represent the uppermost interval of the regressive deposits. Facies evolution in San Valentino does not show a clear facies pattern as in Nago, therefore it cannot be used to support the occurrence of this regressive trend.

The positive oxygen-isotope shift leading to the EOT-1 as seen in TDP Sites 12 and 17 (Step 1, Pearson et al., 2008) has a duration of at least 100 kyr and develops between C4 and C6 (Fig. 7; missing in ODP Site 744 due to core disturbance). Interestingly, in Nago it does not correlate with a sharp sequence boundary but falls within an interval characterized by a stepwise shallowing of the depositional environment between the MFZ and the coralgal framestone. It is probable that this shallowing in Nago is related to a lowering of sea level caused by waxing of continental ice sheets, as evidenced by the positive oxygen-isotope shift leading to the EOT-1 in Tanzania. This gradual lowering of sea level could also explain why it has until now been difficult to locate a sequence boundary related to this event in other localities (Miller et al., 2009). The positive oxygen-isotope shift corresponds to a temperature drop of 2.5 °C (Katz et al., 2008; Miller et al., 2009) and a sea-level fall of 20 to 30 m in St. Stephens Quarry (Alabama) and Priabona (Italy), respectively (Katz et al., 2008; Houben et al., 2012).

Following the EOT-1, a ~0.4‰ negative $\delta^{18}O$ shift occurring at the transition between C6 and C7 is recorded in Tanzania (Fig. 7; missing in ODP Site 744 due to core disturbance). This shift closely coincides with a relative deepening of the environment in Nago. The deepening is recorded above the coralgal framestone, which suddenly stopped growing at around 134 m and is replaced by rocks of Facies 2 and 5 deposited on the middle and outer ramp. Given that the negative oxygen-isotope shift and the deepening trend in Nago seem to be coeval, it is here postulated that a small deglaciation pulse must have occurred between the EOT-1 and Oi-1.

A eustatic sea-level fall is interpreted to have occurred around the Oi-1 (see Miller et al., 2009, for discussion). Based on backstripping on the New Jersey shelf, a sea-level drop between 55 and 105 m is assumed (Kominz and Pekar, 2001; Miller et al., 2005a). Houben et al. (2012) suggest that a sea-level fall of 50 to 60 m, recorded on top of the bryozoan beds in Priabona, was related to the Oi-1. However, no physical evidence for a sequence boundary is found in the corresponding interval in the Nago Formation.

In the pelagic records, the positive $\delta^{18}O$ shift leading to the Oi-1 occurs at the end of the negative $\delta^{13}C$ isotope plateau of segment C7, prior to the positive shift of carbon-isotope values (Fig. 7). At San Valentino, this position is found at the base of the bryozoan limestones (Fig. 4G), which roughly coincides with the LAD of *Discocyclina* (Fig. 2). Unfortunately, the outcrop in Nago ends exactly where the bryozoan beds would be expected. However, exactly the same evolution is observed at other localities in the Lessini Shelf, where bryozoan marls and limestones comprising the level with the extinction of discocyclinids occur just above the Eocene–Oligocene boundary (Fig. 3, Castellarin and Cita, 1969b; Ungaro, 1978; Setiawan, 1983; Barbin, 1988; Brinkhuis, 1994; Trevisani, 1997). The fact that this change in carbonate factory occurred coevally at several localities and that it was accompanied by the extinction of discocyclinids, suggests that it corresponds to an important change in environmental conditions. Bryozoan-dominated deposits can occur below the photic zone (Nebelsick et al., 2005) and this environmental change could thus have been related to a sea-level rise. However, these beds appear simultaneously at several localities in Italy and at different palaeo-water depths. In addition, a simple deepening cannot be responsible for the extinction of discocyclinids, which were important carbonate producers throughout the Eocene and are present in virtually all samples in San Valentino and Nago below the bryozoan beds.

Based on Mg/Ca ratio of benthic foraminifera from St. Stephens Quarry, Wade et al. (2012) propose that a global cooling of ~2 °C occurred around the Oi-1. Quantitative analyses of warm-oceanic vs. cool-oceanic dinocyst distribution in the Massicore resulted in a qualitative sea-surface temperature proxy for the EOT (Houben et al., 2012; Massicore was drilled ca. 100 m away from the Massigano section; Montanari et al., 1994). This proxy shows that a cooling maximum occurred within the upper part of the Gse dinocyst zone, which coincides with the lower part of the bryozoan beds in Priabona (Brinkhuis, 1994) and, consequently, in San Valentino (Fig. 3). According to our stratigraphic scheme this corresponds to the interval of the Oi-1 and thus provides additional evidence for a cooling of ocean waters in the Mediterranean region.

Most of the modern bryozoan carbonates are being produced in cool-water environments (e.g., Mediterranean and southern Australia; James et al., 1997; Pedley and Carannante, 2006; Betzler et al., 2010). Taking into account that a cooling has been reported to occur during the Oi-1, it seems reasonable to interpret the deposition of the bryozoan beds as being mainly driven by a cooling of ocean waters. However, Halfar et al. (2006) described an example of modern bryozoan-dominated deposits forming under eutrophic conditions in warm waters, showing that eutrophic conditions can favour the establishment and dominance of heterotrophic organisms. As minor reductions in surface temperature can represent a several-fold increase in trophic resources (Hallock et al., 1991), it is probable that the relative cooling was accompanied by an increase in nutrient input into shallow environments due to changes in ocean circulation. Moreover, Miller et al. (2009) argue that the formation of a large ice sheet in Antarctica resulted in major perturbations of the thermohaline circulation and ocean upwelling, which in turn could have been responsible for nutrient input into the shallow-marine settings. Thus, although the formation of bryozoan-dominated deposits is here interpreted to be mainly related to cooling of the ocean waters occurring at the Oi-1, it is probable that

nutrients also played a role in the formation of bryozoan facies and in the extinction of oligotrophic larger benthic foraminifera.

6. Conclusions

We present for the first time an integrated biostratigraphic, lithological, and geochemical study of shallow-water carbonates spanning the Late Eocene–earliest Oligocene in the Tethys realm. Calibrated by strontium-isotope stratigraphy and biostratigraphic tie-points, a carbon-isotope stratigraphic correlation between the two studied shallow-water sections (Nago and San Valentino) and three pelagic sections from the Tethys (Massignano), southern Indian Ocean (ODP Site 744), and Tanzania (composite TDP Sites 12 and 17) is proposed. This correlation allows to precisely locate important cooling and glacio-eustatic events occurring at the Eocene–Oligocene greenhouse–icehouse transition and to study their expression in shallow-marine environments.

The Priabonian transgression identified in Nago and San Valentino coincides with a 0.4‰ negative oxygen-isotope shift at ODP Site 744. As no important phase in Alpine tectonics is documented at this time in the Southern Alps, the transgression is interpreted to be associated to a deglaciation pulse producing a glacio-eustatic sea-level rise. This observation confirms previous studies suggesting that smaller transient glaciations in Antarctica occurred already during the Middle and Late Eocene.

The positive oxygen-isotope shift leading to the EOT-1 event is represented in the studied sections by a gradual shallowing of the environment rather than a sharp sequence boundary, which could indicate a gradual build-up of continental ice sheets. The EOT-1 event is followed by a negative shift of around 0.4‰ that corresponds to a relative deepening of the environment in Nago, suggesting a melting pulse between the EOT-1 and the Oi-1.

The positive $\delta^{18}O$ shift leading to the Oi-1 in pelagic records translates in San Valentino into a facies change from red-algal and larger benthic foraminiferal limestones to bryozoan limestones. These bryozoan beds containing the LAD of *Discocyclina* are also found in other Italian localities just above the Eocene–Oligocene boundary. They are interpreted to result from a regional or global cooling pulse occurring at the Oi-1 and are therefore believed to be an analogue of modern cool-water carbonates.

The paucity of documented shallow-marine carbonate deposits spanning the EOT may be partly due to the difficulties to precisely date Late Eocene–Early Oligocene successions. In this sense, a way to overcome this problem and to obtain insight into shallow-marine processes during this important interval of palaeoclimatic and palaeoceanographic changes is the use of a multi-proxy approach combining facies analysis, chemostratigraphy, and biostratigraphy as proposed in this study.

Acknowledgements

This study was supported by the Swiss National Science Foundation grant 20-121545. We are grateful to D. Bassi for introducing us to the Nago section and, together with V. Luciani, providing us with important literature. An earlier version of the manuscript benefited from the careful reading by T. Bover-Arnal. The helpful comments of two anonymous reviewers and journal editor Finn Surlyk were greatly appreciated.

References

Adams, C.G., Butterlin, J., Samanta, B.K., 1986. Larger foraminifera and events at the Eocene/Oligocene boundary in the Indo-West Pacific Region. In: Pomerol, Ch, Premoli Silva, I. (Eds.), Terminal Eocene events: Developments in Palaeontology and Stratigraphy, 9, pp. 237–252.

Agnini, C., Fornaciari, E., Giusberti, L., Grandesso, P., Lanci, L., Luciani, V., Muttoni, G., Pälike, H., Rio, D., Spofforth, D.J.A., 2011. Integrated biomagnetostratigraphy of the Alano section (NE Italy): a proposal for defining the middle–late Eocene boundary. Geological Society of America Bulletin 123, 841–872.

Barbin, V., 1988. The Eocene–Oligocene transition in shallow-water environment: the Priabonian stage type area (Vicentin, Northern Italy). In: Premoli Silva, I., Coccioni, R., Montanari, A. (Eds.), The Eocene–Oligocene boundary in the Marche-Umbria basin (Italy): Special Publication International Subcommission on Paleogene Stratigraphy. IUGS, Ancona, pp. 163–171.

Bassi, D., 1998. Coralline algal facies and their palaeoenvironments in the Late Eocene of Northern Italy (Calcare di Nago, Trento). Facies 39, 179–201.

Beavington-Penney, S.J., Racey, A., 2004. Ecology of extant nummulitids and other larger benthic foraminifera: applications in palaeoenvironmental analysis. Earth-Science Reviews 67, 219–265.

Berggren, W.A., Pearson, P.N., 2005. A revised tropical to subtropical Paleogene planktonic foraminiferal zonation. Journal of Foraminiferal Research 35, 279–298.

Berggren, W.A., Kent, D.V., Swisher, C.C., Aubry, M.P., 1995. A revised Cenozoic geochronology and chronostratigraphy. SEPM Special Publication 54, 129–212.

Betzler, C., Braga, J.C., Jaramillo-Vogel, D., Römer, M., Hübscher, C., Schmiedl, G., Lindhorst, S., 2010. Late Pleistocene and Holocene cool-water carbonates of the Western Mediterranean Sea. Sedimentology 58, 643–669.

Bice, D.M., Montanari, A., 1988. Magnetic stratigraphy of the Massignano section across the Eocene–Oligocene boundary. In: Premoli Silva, I., Coccioni, R., Montanari, A. (Eds.), The Eocene–Oligocene boundary in theMarche-Umbria basin (Italy): Special Publication International Subcommission on Paleogene Stratigraphy. IUGS, Ancona, pp. 111–117.

Blow, W.H., 1979. The Cenozoic Globigerinida: a study of the morphology, taxonomy, evolutionary relationships and the stratigraphical distribution of some Globigerinida (mainly Globigerinacea), 3 vols. E.J. Brill, Leiden (1413 p.).

Bodiselitsch, B., Montanari, A., Koeberl, C., Coccioni, R., 2004. Delayed climate cooling in the Late Eocene caused by multiple impacts: high-resolution geochemical studies at Massignano, Italy. Earth and Planetary Science Letters 223, 283–302.

Boix, C., Frijia, G., Vicedo, V., Bernaus, J.M., Di Lucia, M., Parente, M., Caus, E., 2011. Larger Foraminifera distribution and strontium isotope stratigraphy of the La Cova limestones (Coniacian–Santonian, "Serra del Montsec", Pyrenees, NE Spain. Cretaceous Research 32, 806–822.

Bosellini, A., 1989. Dynamics of Tethyan carbonate platforms. In: Crevello, P.D., Wilson, J.L., Sarg, J.F., Read, J.F. (Eds.), Controls on carbonate platform and basin development: SEPM Special Publication, 44, pp. 3–13.

Bosellini, F.R., 1998. Diversity, composition and structure of Late Eocene shelf-edge coral associations (Nago Limestone, Northern Italy). Facies 39, 203–225.

Brand, U., Veizer, J., 1981. Chemical diagenesis of a multicomponent carbonate system; 2, Stable isotopes. Journal of Sedimentary Research 50, 1219–1236.

Brinkhuis, H., 1994. Late Eocene to Early Oligocene dinoflagellate cysts from the Priabonian type-area (Northeast Italy) — biostratigraphy and paleoenvironmental interpretation. Palaeogeography, Palaeoclimatology, Palaeoecology 107, 121–163.

Brinkhuis, H., Biffi, U., 1993. Dinoflagellate cyst stratigraphy of the Eocene/Oligocene transition in central Italy. Marine Micropaleontology 22, 131–183.

Brinkhuis, H., Visscher, H., 1995. The upper boundary of the Eocene Series: a reappraisal based on dinoflagellate cyst biostratigraphy and sequence stratigraphy. In: Berggren, W.A., Kent, D.V., Swisher, C.C., Aubry, M.P., Hardenbol, J. (Eds.), Geochronology, Time Scales and Global Stratigraphic Correlations: A Unified Temporal Framework for an Historical Geology: SEPM Special Publication, 54, pp. 295–304.

Brown, R.E., Koeberl, C., Montanari, A., Bice, D.M., 2009. Evidence for a change in Milankovitch forcing caused by extraterrestrial events at Massignano, Italy, Eocene–Oligocene boundary GSSP. In: Koeberl, C., Montanari, A. (Eds.), The Late Eocene Earth — hothouse, icehouse and impacts: The Geological Society of America Special Paper, 452, pp. 119–137.

Burla, S., Heimhofer, U., Hochuli, P.A., Weissert, H., Skelton, P., 2008. Changes in sedimentary patterns of coastal and deep-sea successions from the North Atlantic (Portugal) linked to Early Cretaceous environmental change. Palaeogeography, Palaeoclimatology, Palaeoecology 257, 38–57.

Cascella, A., Dinarès-Turell, J., 2009. Integrated calcareous nannofossil biostratigraphy and magnetostratigraphy from the uppermost marine Eocene deposits of the southeastern pyrenean foreland basin: evidences for marine Priabonian deposition. Geologica Acta 7, 281–296.

Castellarin, A., Cita, M.B., 1969a. Calcare di Nago. — Studi Ill. Carta Geologica d'Italia, Formazioni Geologiche, Roma, fascicolo, 2, pp. 49–64.

Castellarin, A., Cita, M.B., 1969b. La coupe priabonienne de Nago (Prov. Trento) et la limite Eocene–Oligocene. Colloque sur l'Eocène, Mémoire du Bureau de recherches Géologiques et Minières (B.R.G.M.), 69, pp. 93–117.

Catuneanu, O., Abreu, V., Bhattacharya, J.P., Blum, M.D., Dalrymple, R.W., Eriksson, P.G., Fielding, C.R., Fisher, W.L., Galloway, W.E., Gibling, M.R., Giles, K.A., Holbrook, J.M., Jordan, R., Kendall, C.G.S.C., Macurda, B., Martinsen, O.J., Miall, A.D., Neal, J.E., Nummedal, D., Pomar, L., Posamentier, H.W., Pratt, B.R., Sarg, J.F., Shanley, K.W., Steel, R.J., Strasser, A., Tucker, M.E., Winker, C., 2009. Towards the standardization of sequence stratigraphy. Earth-Science Reviews 92, 1–33.

Coccioni, R., Monaco, P., Monechi, S., Nocchi, M., Parisi, G., 1988. Biostratigraphy of the Eocene–Oligocene boundary at Massignano (Ancona, Italy). In: Premoli Silva, I., Coccioni, R., Montanari, A. (Eds.), The Eocene–Oligocene boundary in the Marche-Umbria basin (Italy): Special Publication International Subcommission on Paleogene Stratigraphy. IUGS, Ancona, pp. 59–80.

Coccioni, R., Basso, D., Brinkhuis, H., Galeotti, S., Gardin, S., Monechi, S., Spezzaferri, S., 2000. Marine biotic signals across a late Eocene impact layer at Massignano, Italy: evidence for long-term environmental perturbations? Terra Nova 12, 258–263.

Cosovic, V., Drobne, K., Moro, A., 2004. Paleoenvironmental model for Eocene foraminiferal limestones of the Adriatic carbonate platform (Istrian Peninsula). Facies 50, 61–75.

Cotton, L.J., Pearson, P.N., 2011. Extinction of larger benthic foraminifera at the Eocene/Oligocene boundary. Palaeogeography, Palaeoclimatology, Palaeoecology 311, 281–296.

Coxall, H.K., Pearson, P.N., 2007. The Eocene–Oligocene Transition. In: William, M., Haywood, A.M., Gregory, F.J., Schmidt, D.N. (Eds.), Deep-Time Perspectives on Climate Change: Marrying the Signal from Computer Models and Biological Proxies: The Micropaleontological Society, Special Publications, 2, pp. 351–387.
Coxall, H.K., Wilson, P.A., 2011. Early Oligocene glaciation and productivity in the eastern equatorial Pacific: Insights into global carbon cycling. Paleoceanography 26, PA2221. http://dx.doi.org/10.1029/2010PA002021.
Coxall, H.K., Wilson, P.A., Pälike, H., Lear, C.H., Backman, J., 2005. Rapid stepwise onset of Antarctic glaciation and deeper calcite compensation in the Pacific Ocean. Nature 433, 53–57.
Dawber, C.F., Tripati, A.K., Gale, A.S., MacNiocaill, C., Hesselbo, S.P., 2011. Glacioeustasy during the middle Eocene? Insights from the stratigraphy of the Hampshire Basin, UK. Palaeogeography, Palaeoclimatology, Palaeoecology 300, 84–100.
DePaolo, D.J., Ingram, B.L., 1985. High–resolution stratigraphy with strontium isotopes. Science 227, 938–941.
Dickson, J.A.D., Coleman, M.L., 1980. Changes in carbon and oxygen isotope composition during limestone diagenesis. Sedimentology 27, 107–118.
Doglioni, C., Bosellini, A., 1987. Eoalpine and mesoalpine tectonics in the Southern Alps. Geologische Rundschau 76, 735–745.
Embry, A.F., 1993. Transgressive-regressive (TR) sequence analysis of the Jurassic succession of the Sverdrup Basin, Canadian Arctic Archipelago. Canadian Journal of Earth Sciences 30, 301–320.
Fairbanks, R.G., Matthews, R.K., 1978. The marine oxygen isotope record in Pleistocene coral, Barbados, West Indies. Quaternary Research 10, 181–196.
Ferreri, V., Weissert, H., D'Argenio, B., Buonocunto, F.P., 1997. Carbon isotope stratigraphy: a tool for basin to carbonate platform correlation. Terra Nova 9, 57–61.
Frascari, F., 1963. La trasgressione priaboniana nel Vicentino orientale. Giornale di Geologia 30, 219–231.
Frijia, G., Parente, M., 2008. Strontium isotope stratigraphy in the upper Cenomanian shallow-water carbonates of the southern Appennines: Short-term perturbations of marine $^{87}Sr/^{86}Sr$ during the oceanic anoxic event 2. Palaeogeography, Palaeoclimatology, Palaeoecology 261, 15–19.
Gradstein, F.M., Ogg, J.G., Smith, A.G., 2004. A Geologic Time Scale 2004. Cambridge University Press, Cambridge, UK . (589 p.).
Grötsch, J., Billing, I., Vahrenkamp, V., 1998. Carbon isotope stratigraphy in shallow water carbonates: implications for Cretaceous black shale deposition. Sedimentology 45, 623–634.
Halfar, J., Strasser, M., Riegl, B., Godinez-Orta, L., 2006. Oceanography, sedimentology and acoustic mapping of a bryomol carbonate factory in the northern Gulf of California, Mexico. In: Pedley, H.M., Carannante, G. (Eds.), Cool-Water Carbonates: Geological Society, London, Special Publications, 255, pp. 197–215.
Hallock, P., 1979. Trends in test shape with depth in large, symbiont-bearing foraminifera. Journal of Foraminiferal Research 9, 61–69.
Hallock, P., Glenn, E.C., 1986. Large foraminifera: a tool for paleoenvironmental analysis of Cenozoic carbonate depositional facies. Palaios 1, 55–64.
Hallock, P., Premoli Silva, I., Boersma, A., 1991. Similarities between planktonic and larger foraminiferal evolutionary trends through Paleogene paleoceanographic changes. Palaeogeography, Palaeoclimatology, Palaeoecology 83, 49–64.
Hottinger, L., 1997. Shallow benthic foraminiferal assemblages as signals for depth of their deposition and their limitations. Bulletin de la Société Géologique de France 168, 491–505.
Houben, A.J.P., van Mourik, C.A., Montanari, A., Coccioni, R., Brinkhuis, H., 2012. The Eocene–Oligocene transition: Changes in sea level, temperature or both? Palaeogeography, Palaeoclimatology, Palaeoecology 335–336, 75–83.
Huck, S., Heimhofer, U., Rameil, N., Bodin, S., Immenhauser, A., 2011. Strontium and carbon-isotope chronostratigraphy of Barremian–Aptian shoal-water carbonates: Northern Tethyan platform drowning predates OAE 1a. Earth and Planetary Science Letters 304, 547–558.
Hudson, J.D., 1977. Stable isotopes and limestone lithification. Journal of the Geological Society 133, 637–660.
Immenhauser, A., Kenter, J.A.M., Ganssen, G., Bahamonde, J.R., Van Vliet, A., Saher, M.H., 2002. Origin and significance of isotope shifts in Pennsylvanian carbonates (Asturias, NW Spain). Journal of Sedimentary Research 72, 82–94.
James, N.P., 1997. The cool-water carbonate depositional realm. In: James, N.P., Clarke, J.A.D. (Eds.), Cool-Water Carbonates: SEPM Special Publication, 56, pp. 53–76.
James, N.P., Bone, Y., Hageman, S.J., Feary, D.A., Gostin, V.A., 1997. Cool-water carbonate sedimentation during the terminal Quaternary sea-level cycle: Lincoln Shelf, southern Australia. In: James, N.P., Clarke, J.A.D. (Eds.), Cool-water carbonates: SEPM Special Publication, 56, pp. 53–76.
Jenkyns, H.C., 1995. Carbon-isotope stratigraphy and paleoceanographic significance of the Lower Cretaceous shallow-water carbonates of Resolution Guyot, Mid-Pacific Mountains. Proceedings of the Ocean Drilling Program, Scientific Results 143, 99–104.
Jones, C.E., Jenkyns, H.C., Hesselbo, S.P., 1994. Strontium isotopes in Early Jurassic seawater. Geochimica et Cosmochimica Acta 58, 1285–1301.
Jovane, L., Sprovieri, M., Florindo, F., Acton, G., Coccioni, R., Dall'Antonia, B., Dinares-Turell, J., 2007. Eocene–Oligocene paleoceanographic changes in the stratotype section, Massignano, Italy: Clues from rock magnetism and stable isotopes. Journal of Geophysical Research 112, B11101. http://dx.doi.org/10.1029/2007JB004963.
Katz, M.E., Miller, K.G., Wright, J.D., Wade, B.S., Browning, J.V., Cramer, B.S., Rosenthal, Y., 2008. Stepwise transition from the Eocene greenhouse to the Oligocene icehouse. Nature Geoscience 1, 329–334.
Kennett, J.P., Shackleton, N.J., 1976. Oxygen isotopic evidence for the development of the psychrosphere 38 Myr ago. Nature 260, 513–515.
Kiessling, W., Flügel, E., Golonka, J., 2003. Patterns of Phanerozoic carbonate platform sedimentation. Lethaia 36, 195–225.
Kominz, M.A., Pekar, S.F., 2001. Oligocene eustasy from two-dimensional sequence stratigraphic backstripping. Geological Society of America Bulletin 113, 291–304.
Lowrie, W., Lanci, L., 1994. Magnetostratigraphy of Eocene–Oligocene boundary sections in Italy: No evidence for short subchrons within chrons 12R and 13R. Earth and Planetary Science Letters 126, 247–258.
Luciani, V., 1989. Stratigrafia sequenziale del Terziario nella catena del Monte Baldo (Provincie di Verona e Trento). Memorie di Scienze Geologiche 41, 263–351.
Luciani, V., Negri, A., Bassi, D., 2002. The Bartonian–Priabonian transition in the Mossano section (Colli Berici, north-eastern Italy): a tentative correlation between calcareous plankton and shallow-water benthic zonations. Geobios 35, 140–149.
Marshall, J.D., 1992. Climatic and oceanographic isotopic signals from the carbonate rock record and their preservation. Geological Magazine 129, 143–160.
Martini, E., 1971. Standard Tertiary and Quaternary calcareous nannoplankton zonation. In: Farinacci, A. (Ed.), Proceedings of the Second Planktonic Coference, Rome, pp. 739–785.
McArthur, J.M., 1994. Recent trends in strontium isotope stratigraphy. Terra Nova 6, 331–358.
McArthur, J.M., Howarth, R.J., Bailey, T.R., 2001. Strontium isotope stratigraphy: LOWESS Version 3: Best fit to the marine Sr-isotope curve for 0–509 Ma and accompanying look-up table for deriving numerical age. Journal of Geology 109, 155–170.
McArthur, J.M., Mutterlose, J., Price, G.D., Rawson, P.F., Ruffell, A., Thirlwall, M., 2004. Belemnites of Valanginian, Hauterivian and Barremian age: Sr isotope stratigraphy, composition ($^{87}Sr/^{86}Sr$, $\delta^{13}C$, $\delta^{18}O$, Na, Sr, Mg), and palaeo-oceanography. Palaeogeography, Palaeoclimatology, Palaeoecology 202, 253–272.
Menegatti, A.P., Weissert, H., Brown, R.S., Tyson, R.V., Farrimond, P., Strasser, A., Caron, M., 1998. High-resolution ^{13}C stratigraphy through the early Aptian "Livello Selli" of the Alpine Tethys. Paleoceanography 13, 530–545.
Meulenkamp, J.E., Sissingh, W., 2003. Tertiary palaeogeography and tectonostratigraphic evolution of the Northern and Southern Peri-Tethys platforms and the intermediate domains of the African-Eurasian convergent plate boundary zone. Palaeogeography, Palaeoclimatology, Palaeoecology 196, 209–228.
Miller, K.G., Wright, J.D., Fairbanks, R.G., 1991. Unlocking the Ice House: Oligocene–Miocene oxygen isotopes, eustasy, and margin erosion. Journal of Geophysical Research 96, 6829–6848.
Miller, K.G., Kominz, M.A., Browning, J.V., Wright, J.D., Mountain, G.S., Katz, M.E., Sugarman, P.J., Cramer, B.S., Christie-Blick, N., Pekar, S.F., 2005a. The phanerozoic record of global sea-level change. Science 310, 1293–1298.
Miller, K.G., Wright, J.D., Browning, J.V., 2005b. Visions of ice sheets in a greenhouse world. Marine Geology 217, 215–231.
Miller, K.G., Browning, J.V., Aubry, M.-P., Wade, B.S., Katz, M.E., Kulpecz, A.A., Wright, J.D., 2008. Eocene–Oligocene global climate and sea-level changes: St. Stephens Quarry, Alabama. Geological Society of America Bulletin 120, 34–53.
Miller, K.G., Wright, J.D., Katz, M.E., Wade, B.S., Browning, J.V., Cramer, B.S., Rosenthal, Y., 2009. Climate threshold at the Eocene–Oligocene transition: Antarctic ice sheet influence on ocean circulation. In: Koeberl, C., Montanari, A. (Eds.), Late Eocene Earth: Hothouse, Icehouse, and Impacts: Geological Society of America Special Papers, 452, pp. 169–178.
Montanari, A., Sandroni, P., Clymer, A., Collins, G., Coccioni, R., Lanci, L., Lowrie, W., 1994. The MASSICORE: preliminary report on a core drilled across the Eocene–Oligocene boundary in the type locality of Massignano (Italy). Bulletin of Liaison and Information, International Geological Correlation Project 196, 13–16.
Mutti, M., John, C.M., Knoerich, A.C., 2006. Chemostratigraphy in Miocene heterozoan carbonate settings: applications, limitations and perspectives. In: Pedley, H.M., Carannante, G. (Eds.), Cool-Water Carbonates: Geological Society, London, Special Publications, 255, pp. 307–322.
Nebelsick, J.H., Rasser, M.W., Bassi, D., 2005. Facies dynamics in Eocene to Oligocene circumalpine carbonates. Facies 51, 197–217.
Nocchi, M., Monechi, S., Coccioni, R., Madile, M., Monaco, P., Orlando, M., Parisi, G., Premoli Silva, I., 1988. The extinction of Hantkeninidae as a marker for recognizing the Eocene–Oligocene boundary: a proposal. In: Premoli Silva, I., Coccioni, R., Montanari, A. (Eds.), The Eocene–Oligocene boundary in the Marche-Umbria basin (Italy): Special Publication International Subcommission on Paleogene Stratigraphy. IUGS, Ancona, pp. 249–252.
Papazzoni, C.A., Sirotti, A., 1995. Nummulite biostratigraphy at the Middle/Upper Eocene boundary in the Northern Mediterranean area. Rivista Italiana di Paleontologia e Stratigrafia 101, 63–80.
Parente, M., Frijia, G., Di Lucia, M., 2007. Carbon-isotope stratigraphy of Cenomanian–Turonian platform carbonates from the southern Apennines (Italy): a chemostratigraphic approach to the problem of correlation between shallow-water and deep-water successions. Journal of the Geological Society 164, 609–620.
Pearson, P.N., McMillan, I.K., Wade, B.S., Jones, T.D., Coxall, H.K., Bown, P.R., Lear, C.H., 2008. Extinction and environmental change across the Eocene–Oligocene boundary in Tanzania. Geology 36, 179–182.
Pedley, M., Carannante, G., 2006. Cool-water carbonate ramps: a review. In: Pedley, H.M., Carannante, G. (Eds.), Cool-Water Carbonates: Geological Society, London, Special Publications, 255, pp. 1–9.
Pekar, S.F., Christie-Blick, N., Kominz, M.A., Miller, K.G., 2002. Calibration between eustatic estimates from backstripping and oxygen isotopic records for the Oligocene. Geology 30, 903–906.
Peters, S.E., Carlson, A.E., Kelly, D.C., Gingerich, P.D., 2010. Large-scale glaciation and deglaciation of Antarctica during the Late Eocene. Geology 38, 723–726.
Poag, C.W., Mankinen, E., Norris, R.D., 2003. Late Eocene impacts: Geologic record, correlation, and paleoenvironmental consequences. In: Prothero, D.R., Ivany, L.C., Nesbitt, E.A. (Eds.), Greenhouse to Icehouse: The Marine Eocene–Oligocene Transition. Columbia University Press, New York, pp. 495–510.

Premoli Silva, I., Jenkins, D.G., 1993. Decision on the Eocene–Oligocene boundary stratotype. Episodes 16, 379–382.
Salamy, K.A., Zachos, J.C., 1999. Latest Eocene–Early Oligocene climate change and Southern Ocean fertility: inferences from sediment accumulation and stable isotope data. Palaeogeography, Palaeoclimatology, Palaeoecology 145, 61–77.
Schneider, S., Franz, T.F., Werner, W., 2009. Sr-isotope stratigraphy of the Upper Jurassic of central Portugal (Lusitanian Basin) based on oyster shells. International Journal of Earth Sciences (Geologische Rundschau) 98, 1949–1970.
Serra-Kiel, J., Hottinger, L., Caus, E., Drobne, K., Ferrandez, C., Jauhri, A.K., Less, G., Pavlovec, R., Pignatti, J., Samso, J.M., Schaub, H., Sirel, E., Strougo, A., Tambareau, Y., Tosquella, J., Zakrevskaya, E., 1998. Larger foraminiferal biostratigraphy of the Tethyan Paleocene and Eocene. Bulletin de la Société Géologique de France 169, 281–299.
Setiawan, J.R., 1983. Foraminifera and microfacies of the type Priabonian. Utrecht Micropaleontological Bulletins 29, 161p.
Spezzaferri, S., Basso, D., Coccioni, R., 2002. Late Eocene planktonic foraminiferal response to an extraterrestrial impact at Massignano GSSP (northeastern Appennines, Italy). Journal of Foraminiferal Research 32, 188–199.
Steuber, T., 2003. Strontium isotope chemostratigraphy of rudist bivalves and Cretaceous carbonate platforms. In: Gili, E., Negra, M.H., Skelton, P.W. (Eds.), North African Cretaceous Carbonate Platform Systems. : NATO Science Series, Earth and Environmental Sciences 28. Kluwer Academic, Dordrecht, pp. 229–238.
Steuber, T., Korbar, T., Jelaska, V., Gušić, I., 2005. Strontium-isotope stratigraphy of Upper Cretaceous platform carbonates of the island of Brac (Adriatic Sea, Croatia): implications for global correlation of platform evolution and biostratigraphy. Cretaceous Research 26, 741–756.
Steuber, T., Parente, M., Hagmaier, M., Immenhauser, A., van der Kooij, B., Frijia, G., 2007. Latest Maastrichtian species-rich rudist associations of the Apulian Margin of Salento (S Italy) and the Ionian Islands (Greece). In: Scott, R.W. (Ed.), Cretaceous Rudists and Carbonate Platforms: Environmental Feedback: SEPM Special publication, 87, pp. 151–157.
Stoll, H.M., Schrag, D.P., 2000. High-resolution stable isotope records from the Upper Cretaceous rocks of Italy and Spain: Glacial episodes in a greenhouse planet? Geological Society of America Bulletin 112, 308.
Strasser, A., Pittet, B., Hillgärtner, H., Pasquier, J.-B., 1999. Depositional sequences in shallow carbonate-dominated sedimentary systems: concepts for a high-resolution analysis. Sedimentary Geology 128, 201–221.
Swart, P.K., 2008. Global synchronous changes in the carbon isotopic composition of carbonate sediments unrelated to changes in the global carbon cycle. Proceedings of the National Academy of Sciences of the United States of America 105, 13741–13745.
Trevisani, E., 1997. Il margine settentrionale del Lessini Shelf: Evoluzione paleogeografica e dinamica deposizionale del paleogene della Valsugana (Trentino Sud-Orientale). Atti Ticinesi di Scienze della Terra 5, 115–127.
Tripati, A., Backman, J., Elderfield, H., Ferretti, P., 2005. Eocene bipolar glaciation associated with global carbon cycle changes. Nature 436, 341–346.
Ungaro, S., 1969. Étude micropaléontologique et stratigraphique de l'Eocène supérieur (Priabonien) de Mossano (Colli Berici). Colloque sur l'Eocène, Mémoire du Bureau de recherches Géologiques et Minières (B.R.G.M.), 69, pp. 267–280.
Ungaro, S., 1978. L'Oligocene dei Colli Berici. Rivista Italiana di Paleontologia e Stratigrafia 84, 199–278.
Ungaro, S., Bosellini, A., 1965. Studio micropaleontologico e stratigrafico: sul limite Eocene–Oligocene nei Colli Berici occidentali. Annali dell'Università degli Studi di Ferrara 3, 157–183.
Vahrenkamp, V.C., 1996. Carbon isotope stratigraphy of the Upper Kharaib and Shuaiba Formations: implications for the Early Cretaceous evolution of the Arabian Gulf region. AAPG Bulletin 80, 647–662.
Veizer, J., 1983. Trace elements and isotopes in sedimentary carbonates. Reviews in Mineralogy 11, 265–299.
Vonhof, H.B., Smit, J., Brinkhuis, H., Montanari, A., Nederbragt, A.J., 2000. Global cooling accelerated by early late Eocene impacts? Geology 28, 687–690.
Wade, B.S., Houben, A.J.P., Quaijtaal, W., Schouten, S., Rosenthal, Y., Miller, K.G., Katz, M.E., Wright, J.D., Brinkhuis, H., 2012. Multiproxy record of abrupt sea-surface cooling across the Eocene–Oligocene transition in the Gulf of Mexico. Geology 40, 159–162.
Wissler, L., Funk, H., Weissert, H., 2003. Response of Early Cretaceous carbonate platforms to changes in atmospheric carbon dioxide levels. Palaeogeography, Palaeoclimatology, Palaeoecology 200, 187–205.
Zachos, J.C., Quinn, T.M., Salamy, K.A., 1996. High-resolution (104 years) deep-sea foraminiferal stable isotope records of the Eocene–Oligocene climate transition. Paleoceanography 11, 251–266.
Zachos, J.C., Pagani, M., Sloan, L., Thomas, E., Billups, K., 2001. Trends, rhythms, and aberrations in global climate 65 Ma to present. Science 292, 686–693.